SAPIENZA
UNIVERSITÀ DI ROMA

Characterization of the transcriptional complexes enrolled by Yes-associated protein (YAP) in hepatoma cells and their regulation by ERK5/MAPK

PhD program in "Genetics and Human Biology" – XXXVI Cycle

Candidate:

Veronica Consalvi

Tutors:

Prof.ssa Laura Amicone

Prof.ssa Alessandra Marchetti

Coordinator:

Prof.ssa Laura Stronati

SUMMARY

ABSTRACT

The transcriptional cofactor Yes-Associated Protein (YAP) is known to be a master regulator of gene expression programs involved in several cell functions. It cooperates with several transcriptional factors, mainly with those belonging to the TEAD family. There is increasing evidence that the composition and genomic occupancy of YAP-recruiting transcriptional complexes may depend on tissue and cellular context, thus dynamically driving specific gene expression and different functional outcomes. The formation and specific composition of these complexes may be regulated by the phosphorylation status of the components, which eventually depends on the activity of enzymes belonging to different signaling pathways. Based on our recent work identifying the transcriptional factor STAT3 as a new interactor of YAP in liver cells and ERK5 as a new regulator of YAP activity, and on recent literature data showing lncRNAs as functional components of transcriptional molecular platforms, this PhD project aimed to the structural and functional characterization of YAP-enrolled transcriptional complexes in transformed liver cells also focusing on their upstream regulation. Specifically, I have i) investigated the role

of STAT3 in the YAP-dependent gene expression, ii) analyzed the mechanistic and functional role of ERK5/MAPK in the control of the assembly/activity of YAP/STAT3 and YAP/TEAD complexes and of their recruitment on DNA, and iii) evaluated lncRNA MALAT1 as potential functional member of YAP-dependent transcriptional platforms. Provided data demonstrated that, in hepatoma cells, i) STAT3 regulates YAP transcriptional activity by cooperating with TEAD on previously characterized YAP/TEAD target genes (i.e. *Ctgf* and *Cyr61*); ii) YAP/STAT3 DNA binding is dependent on ERK5 kinase activity; iii) YAP is a new direct target of ERK5 kinase activity. Furthermore, we gathered evidence that lncRNA MALAT1 physically interacts with YAP in an ERK5-dependent manner and that it is required for YAP-target gene expression. On the basis of these results, a model for the dynamic formation and activation of YAP/STAT3/TEAD transcriptional complex has been proposed for CTGF promoter, extendable to other YAP target genes and possibly involving other components, including MALAT1.

Overall, our findings provide a possible paradigm of how specific YAP-including transcriptional complexes can be dynamically assembled and drive specific YAP-dependent gene

expression and cellular outcomes.

In perspective, these studies may pave the way to new therapeutic approaches, aimed at interfering with YAP activity in pathologies where it has been found deregulated.

INTRODUCTION

YAP

YAP (Yes-associated protein) is a transcriptional cofactor that plays a role in the physiology of many organs and tissues by regulating the expression of numerous genes involved in processes such as proliferation, differentiation, homeostasis and stemness maintenance (Varelas et al., 2014).

It acts as a pro-oncogenic factor and YAP overexpression or constitutive activity is associated with many human cancers (Zanconato F et al., 2016).

YAP is closely related to TAZ, another transcriptional co-factor with which it forms a dimeric complex (Varelas et al., 2014). To perform its function, the YAP/TAZ complex, which lacks DNA-binding domains, binds transcription factors, primarily those belonging to the TEAD family (Varelas et al., 2014). However, several studies document the association between YAP/TAZ and other transcription factors, downstream effectors of different signaling pathways, determining cell- and context-dependent gene expression and cellular outcomes.

Mechanistically, the regulation of gene expression by YAP and

TFs can occur in several ways (Figure 1):

1. YAP/TAZ can be shared by different TFs whose binding sites localize on proximal or distal regulatory regions, such as AP-1 or MRTF/SRF (Zanconato et al., 2015; Liu et al., 2016).
2. Transcription factors can enhance the binding of YAP/TAZ to TEAD consensus sites. It is the case of MYC that promotes the recruitment of YAP/TAZ at genomic loci constitutively occupied by TEAD (Croci et al., 2017).
3. Transcription factors may be recruited by YAP/TAZ-TEAD, independently from the presence of their binding motif on DNA, as seen in the case of ZEB1 (Lehmann et al., 2016). The resulting transcriptional complexes, whose formation mechanism is still under investigation, drive the activation of specific gene subsets.
4. YAP/TAZ can regulate transcription in a TEAD-independent manner. It is evident in its interaction with p73 and mutant p53 in the regulation of DNA damage response and cell proliferation, respectively, where YAP/TAZ acts as transcriptional modulator of the TF-dependent gene expression (Levy et al., 2007; Di Agostino et al., 2016).
5. Protein-protein interaction between YAP/TAZ and TFs can

occur in a chromatin-independent manner in a cytoplasmic cross–talk with different signaling pathways. This is exemplified by β-catenin and YAP/TAZ, both components of the WNT disruption complex, or by the cytoplasmic association of YAP/TAZ with SMADs (Varelas et al., 2010; Heallen et al., 2011).

YAP-including transcriptional complexes can recruit chromatin modifiers to drive the activation or inhibition of gene expression. Regarding the YAP/TEAD complex, it can directly (or indirectly) recruit the chromatin modifier complex SWI/SNF and the H3K4 methyltransferase NcoA6, which activates the transcription of several target genes. The most well-known of these genes are CTGF and Cry61 (Oh et al., 2013; Oh et al., 2014; Qing et al., 2014; Skibinski et al., 2014).

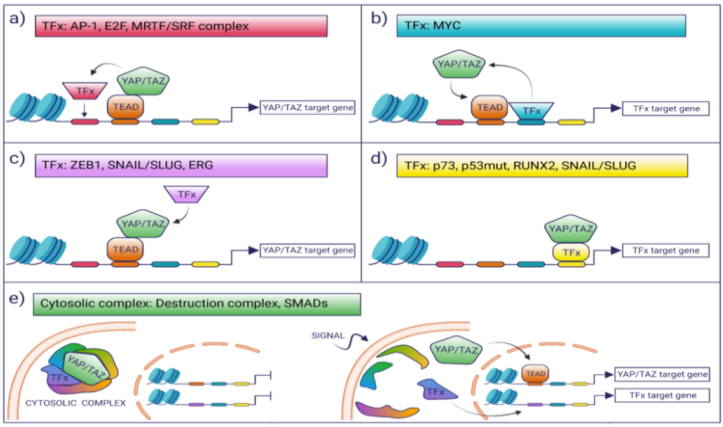

Figure 1. *Depiction of the molecular complexes through which YAP controls the transcription of various target genes* (*Lopez-Hernandez A et al., 2021)*

On the other hand, YAP/TAZ-including transcriptional complexes, can recruit the NuRD complex to block the expression of genes such as DDIT4 and Trail (Kim M. et al., 2015). Notably, YAP can also indirectly influence gene expression, by interacting in the cytoplasm with specific molecules and interfering with signaling pathways (i.e., by sequestering DVL2, YAP can interfere with Wnt-dependent gene expression) (Gan X.Q. & Wang, 2008; Itoh et al., 2005).

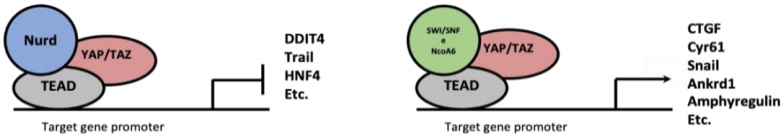

Figure 2. *Depiction of the molecular complexes through which YAP controls the transcription of various target genes (elaboration of Kim M. et al., 2015).*

1.1 YAP in tissue homeostasis and differentiation.

YAP subcellular localization correlates with the proliferation rate and differentiation state of several cell types. Generally, it is localized in the nucleus and transcriptionally active in proliferating and undifferentiated cells, while it is confined to the cytoplasm or strongly downregulated in terminally differentiated cells. However, a nuclear and active YAP may be associated with specific cellular differentiation programs.

YAP plays a role in maintaining the stem compartment or switching on the differentiation program in the cellular system of intestinal crypts.

In particular, the Wnt pathway is the primary driver of self-renewal and tissue regeneration in the intestine. Downregulation of this pathway results in the loss of intestinal

crypts. At the same time, upregulation following tissue damage leads to tissue hyperplasia, expansion of intestinal stem cells (ISCs), and the formation of ectopic crypts and micro-adenomas (Barry et al., 2013; Pinto et al., 2003).

In the intestine, YAP is present in the nucleus of intestinal stem cells (ISCs), where the Wnt pathway is active. Conversely, it localizes to the cytoplasm in the intestinal villi, where the Wnt pathway is reduced (Cai et al., 2010; Silvis et al., 2011). In intestinal stem cells and cells undergoing post-inflammation regeneration, YAP interacts with beta-catenin, creating a transcriptional complex that translocates into the nucleus and activates specific cell proliferation gene programs (Gregorieff et al., 2015). During the differentiation process, instead, YAP is localized in the cytoplasm, where it sequesters the downstream Wnt mediator DVL2 (Gan X.Q. & Wang, 2008; Itoh et al., 2005). YAP-mediated inactivation of DVL2 and the inactivation of the Wnt-dependent gene expression causes a reduction in gut length and crypt diameter (Metcalfe et al., 2010). Accordingly, Barry et al. (2013) revealed the YAP-dependent Wnt pathway downregulation as a pivotal element of the transition from a stem to a differentiated state of the cells (Barry et al., 2013).

The epidermis is another tissue where YAP plays a central role

in cell proliferation and tissue homeostasis maintenance. It is a stratified squamous epithelium that renews and repairs wounds through stem cells at the basement membrane level. YAP is nuclear and transcriptionally active in these cells and promotes cell proliferation in the tissue renewal process. Elevation of the YAP level induces cell proliferation during wound healing and is observed during tumor formation. (Elbediwy et al., 2016).

In the adult liver, YAP is nuclear in a subpopulation of bile duct cells expressing markers of liver progenitors, while it is at a deficient level and located in the cytoplasm in hepatocytes (Li H. et al., 2012; Zhang N. et al., 2010). Overexpression of YAP in bile duct cells leads to hyperplasia of the ductal compartment. Meanwhile, in hepatocytes, it leads to dedifferentiation toward liver progenitor cells and ultimately to liver overgrowth (Yimlamai et al., 2014).

Additional evidence supporting the role of YAP in liver cell differentiation comes from its impact on the dynamic genome redistribution of key hepatocyte differentiation factors during liver differentiation, including HNF4 and FOX2A. These transcription factors interact with thousands of enhancer sequences to guide embryonic liver development and achieve

mature, functional hepatocytes. Alder and his research group used genetically modified mice carrying the pharmacologically inducible YAP gene to demonstrate that this transcriptional co-factor negatively regulates the expression of hepatocyte genes while increasing the expression of typical hepatoblast genes by influencing the general redistribution of master regulators on hepato-specific regulatory sequences (Alder et al., 2014).

Recent data obtained in my laboratory, also with my contribution, have unveiled a novel molecular mechanism by which YAP can control hepatocyte differentiation. In this context, YAP has been characterized as a new member of a previously identified molecular circuit of reciprocal transcriptional inhibition between the master factor of EMT/stemness Snail and MET/hepatocyte differentiation HNF4α (Figure 3). In particular, we found YAP as a target of the negative and positive control of HNF4α and Snail, respectively; on the other hand, it acts as a positive and negative controller of Snail and HNF4α (Noce et al., 2019).

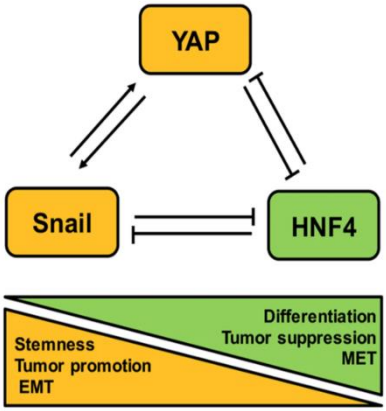

Figure 3. *The molecular circuit controlling stemness/differentiation in liver cells is based on the reciprocal regulation between YAP, Snail, and HNF4 proteins (Noce et al., 2019).*

As reported above, the differentiation process is not always correlated with cytoplasmic retention and inactivation of YAP. For example, during the differentiation of astrocytic cells YAP is localized into the nucleus where, downstream of the BMP2 pathway, it is required for SMAD1 protein stability (Huang et al., 2016). Moreover, the differentiation of mesenchymal stem cells toward the osteogenic lineage depends on the nuclear YAP that interacts with and stabilizes beta-catenin (Jun-Xiu Pan,2018).

1.2 YAP in oncogenesis

YAP dysregulation is common in various cancers of different tissue origins. Specifically, lung, colon, breast, and ovarian cancer cells often exhibit over-expression and nuclear accumulation of YAP and TAZ (Cao et al., 2017; Zanconato et al., 2016). High YAP activity is often associated with poor prognosis and resistance to different therapeutic approaches, such as chemotherapy, radiation, and targeted therapies. It can drive cancer cell proliferation, invasion and metastasis (Zanconato et al., 2016). Over-expression of YAP/TAZ is associated with resistance to apoptosis and increased numbers of cancer stem cells (Cordenonsi et al., 2011; Chan Wee et al., 2008).

In cancer tissues, the activation of YAP/TAZ in cancer-associated fibroblasts promotes the expression of extracellular matrix (ECM) proteins, such as laminin and fibronectin. It induces increased ECM stiffness and contributes to the maintenance of cancer stem cells and cancer-associated fibroblasts (Calvo et al., 2013).

Cell invasion and metastasis are common characteristics of cancer cells. YAP strongly promotes these activities. High expression levels of YAP in cancer cells lead to the epithelial-

mesenchymal transition (EMT), which involves reprogramming of gene expression, loss of cell-cell adhesions and apicobasal polarity, and acquisition of motility. Overexpression of YAP in normal cells does not induce EMT, indicating that YAP is not the master gene of the process. It suggests that YAP may cooperate and act synergistically with other cancer-associated genes (Bai et al., 2016; Shao et al., 2014).

1.3 The regulation of YAP/TAZ by the Hippo pathway

YAP protein is the downstream effector of the Hippo pathway, inhibitory signaling that responds to mechanical and biochemical stimuli from the cellular microenvironment. The Hippo pathway is evolutionarily conserved from Drosophila to mammals (Mo J. et al., 2014). Its activation involves a cascade of molecular events in which the phosphorylation and activation of the Ser/Thr kinase LATS1/2 plays a crucial role. LATS1/2 phosphorylates YAP on residues S127 and S381, promoting its cytoplasmic sequestration or proteasome-mediated degradation (Pan et al., 2010; Varelas et al., 2014). Therefore, an active Hippo pathway leads to the functional inactivation of the

YAP protein. In contrast, if the LATS1/2 kinase is not activated, YAP can translocate into the nucleus to perform its function on DNA through the interaction with transcriptional factors (Zhao Bin et al., 2008; Varelas et al., 2014).

LATS1/2 activation is typically dependent on the MST1/2 kinase-induced phosphorylation (Hippo in *Drosophila*), although there is growing evidence for alternative MST1/2-independent activating pathways (Harvey et al., 2013; Yin et al., 2013).

Several molecular mechanisms can modulate the Hippo pathway and YAP/TAZ activity. Regarding epithelial cells, evidence suggests that proteins belonging to cell-cell junction complexes play a crucial role in regulating the Hippo pathway (Moroishi et al., 2015). The basolateral junction protein Scribble (SCRIB) is essential in facilitating the activation of MST and LATS kinases, leading to the cytoplasmic retention and functional inhibition of YAP/TAZ. In adherent cells, YAP and TAZ localize to the cytoplasmic level. However, the loss of cell-cell adhesions and cell polarity can induce a different localization of YAP/TAZ. The reduction of SCRIB activity on MST and LATS kinases, due to its delocalization from the membrane, leads to the nuclear translocation of YAP/TAZ and

the activation of specific transcriptional profiles (Cordenonsi et al., 2011; Zhao Bin et al., 2007).

Neurofibromin 2 (NF2) is another membrane protein with a significant role in transducing extracellular signals that regulate the Hippo pathway in epithelial cells. When localized in the membrane, NF2 interacts with several proteins, including alpha-catenin and Angiomotin (AMOT), and coordinates the activation of LATS kinases, making it a potent tumor suppressor (Yin et al., 2013).

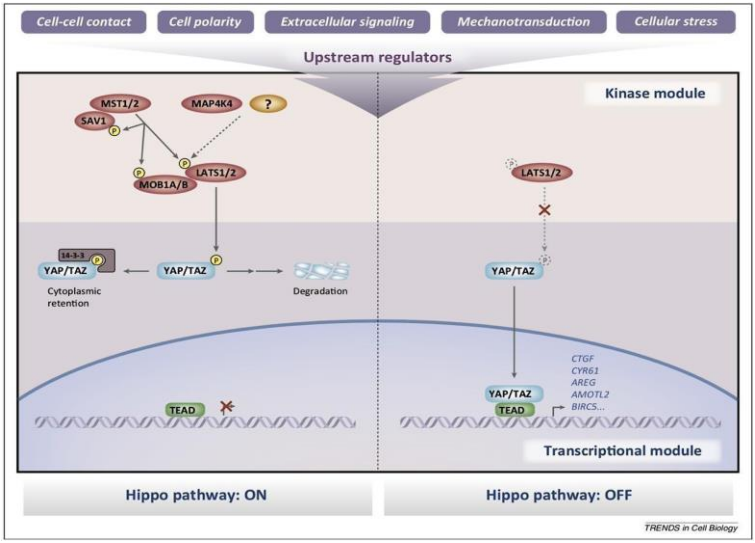

Figure 4. *Hippo pathway (Moroishi et al., 2015)*

NF2 can negatively affect YAP activation even when it is not localized to the membrane, by interfering with the ubiquitin-dependent and proteasome-mediated degradation of LATS. This interference occurs through the binding to the ubiquitin ligase CRL4-DCAF1, which targets LATS specifically (Wilson et al., 2014).

In addition to LATS1/2 kinases, YAP and TAZ can be inhibited by upstream regulators of the Hippo pathway, such as AMOT, Tyrosine Phosphatase 14 (PTPN14), and alpha-catenin. These regulators sequester YAP and TAZ, preventing their access to the nucleus. AMOT is an actin filament-binding protein that mainly localizes at occluding junctions (Mana-Capelli et al., 2014).

A recent study found that LATS1/2 kinases can enhance the inhibitory activity of AMOT by phosphorylating the binding domain present in actin filaments. This activity blocks AMOT-actin filament binding by promoting YAP binding and sequestration (Adler et al., 2013; Dai et al., 2013; Mana-Capelli et al., 2014). Therefore, LATS1/2 kinases can directly and indirectly inhibit YAP activity and nuclear localization. PTPN14 interacts directly with the WW domains of YAP using PPxY motifs, sequestering YAP in the cytoplasm (Liu et al., 2013;

Wang W. et al., 2015). The protein alpha-catenin, associated with the adherens junctions, regulates YAP by sequestering the phosphorylated YAP/14-3-3 complex into the cytoplasm. Therefore, YAP inhibition is a mechanism that strictly depends on its phosphorylation (Schlegelmilch et al., 2011).

1.4 Hippo-independent YAP activating pathways

For years, it was believed that the mechanism of YAP activation in cancer was almost exclusively due to the 'switching off' of the Hippo pathway (Pan et al., 2010; Meng et al., 2016). However, mutations that inactivate the Hippo pathway are rare in human tumors (Harvey et al., 2013). In mouse models where the pathway is experimentally inactivated, tumor onset occurs at a lower rate and after a much longer latency than in YAP over-expressing mice (Zanconato et al., 2016). These findings suggest that Hippo signaling cannot be considered the sole regulatory pathway of YAP.

Although most evidence for Hippo-independent regulatory elements of YAP has been collected in cancer, indications of alternative activation pathways have also been obtained in

various biological processes. It is important to note that these findings are not limited to the upstream portion of the LATS1/2 kinase signaling pathway. A growing body of data indicates that conditions associated with active YAP, such as treatment with growth factors, mechanical stimulation, or neoplastic transformation of the cell, are characterized by mechanisms independent from Hippo kinase but LATS1/2-dependent or entirely Hippo signaling-independent (Feng et al., 2014; Kim N. et al., 2011; Meng et al., 2015; Z. Zhang et al., 2010).

Signaling pathways that can activate YAP independently of Hippo or MST1/2 include those involving Rho family GTPases, SRC/Yes, and those originating from G-protein-associated receptors (Yu et al., 2012).

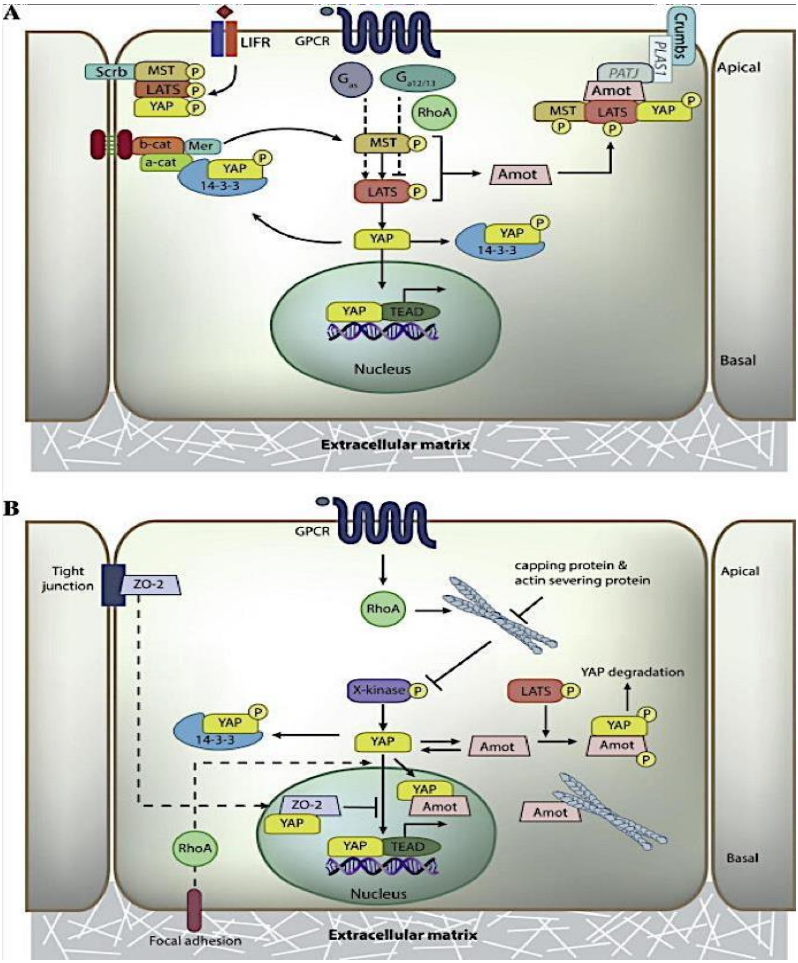

Figure 5. *Hippo's canonical (A) and noncanonical (B) pathways (Low et al., 2014)*

MAPK ERK5

The ERK5/BMK1 protein belongs to the conventional MAPK family and shares many structural and functional features with other MAPKs. However, it is approximately twice the size due to a single domain at the C-terminal end, to which a transcriptional transactivation function has been ascribed (TAD domain in Fig. 5).

ERK5 was initially identified as a MAPK activated by oxidative stress. It has since been found downstream of pathways activated by mitogens (such as EGF, NGF, and FGF), cytokines (such as LIF, IL-6, and TGFbeta), and mechanical stress (such as shear stress) (Abe et al., 1996; Drew et al., 2012; Marchetti et al., 2008; Yan et al., 1999).

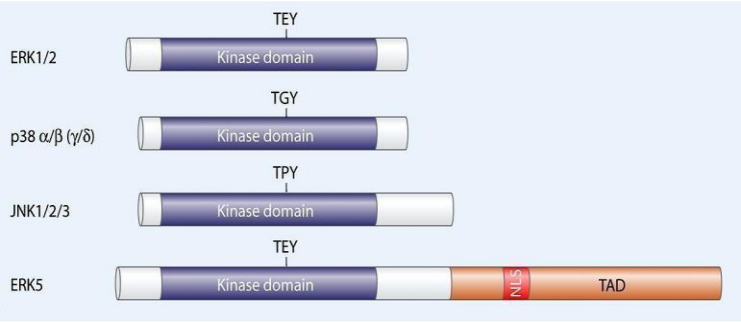

Figure 6. *A schematic representation of the structure of conventional MAPKs.*

All MAPKs have a Ser/Thr kinase domain that is well-preserved and is flanked by N- and C-terminal regions of different length. ERK5 has a unique C-terminal, including a transcriptional transactivation domain (TAD) and a nuclear localization signal (NLS).

Like other MAPKs, ERK5 is activated through the cascade of phosphorylations including Ras or Src, the MAPKKK MEKK2/MEKK3 and a specific MAPKK MEK5, which phosphorylates the Thr218 and Tyr220 residues at the TEY sequence of ERK5. This allows its autophosphorylation at the C-terminal level, leading to its activation.

Phosphorylation by MEK5 also regulates the subcellular localization of the protein by inducing a conformational change that exposes the nuclear localization signal (NLS), allowing for translocation into the nucleus (Morimoto et al., 2007).

MEKK2 and MEKK3 are not specific to the ERK5 pathway, but MEK5 is the only MAPKK that precisely and non-redundantly activates ERK5. As ERK5 is the only known substrate of MEK5, all effects of MEK5 have been attributed to its ability to activate ERK5.

Upon activation and import into the nucleus, ERK5 phosphorylates and directly activates several transcription factors, including members of the MEF2 family of factors (myocyte enhancer factor 2A, 2C, and 2D), Sap1a, c-fos, c-Myc, Bad, and other kinases such as SGK, GSK3**β** and p90RSK (Kamakura et al., 1999; Kato et al.,

1997; Terasawa et al., 2003) (Figure 6).

ERK5 activity extends beyond its kinase function. It can activate transcription factors through phosphorylation and act as their co-activator through the C-terminal domain (Kasler et al., 2000; Kato et al., 1997). However, efficient transcriptional activation of target genes (e.g. MEF2) requires the TAD domain (Kasler et al., 2000). The significance of the TAD domain is evident from the fact that even ERK5 forms that are catalytically inactive but forcibly retained in the nucleus (as observed in many cancer cells) can still bind transcription factors and regulate their transcriptional activity (Erazo et al., 2013). Therefore, the most reliable approach to investigate ERK5 activation is to measure and quantify the activity of its phosphorylation substrates, particularly MEF2, on specific promoters controlling a reporter gene expression (Bliss et al., 2012).

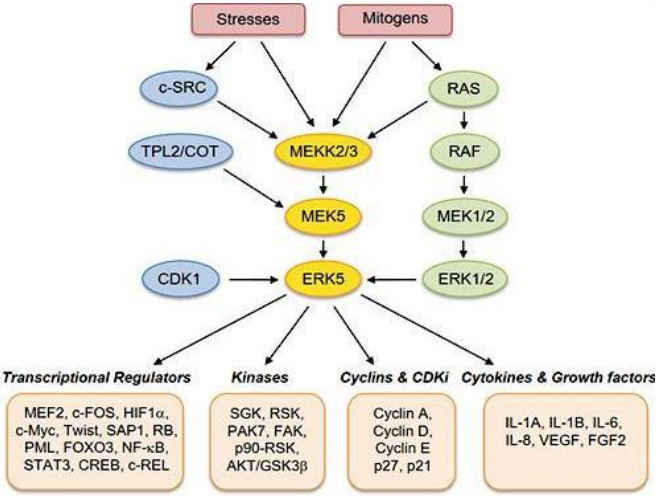

Figure 7. *Activators and targets of ERK5 protein (Stecca et al., 2019)*

2.1 ERK5 functions

ERK5 regulates several cellular processes, such as proliferation, survival, angiogenesis, differentiation, EMT, and cancer onset and/or progression (Drew et al., 2012) (Figure 7).

ERK5 knock-out studies in mice have shown a role of the kinase in embryonic development, particularly in muscle, neuronal, and endothelial differentiation. The loss of ERK5 function leads to animal death during development, primarily due to angiogenesis failure, reduced neuronal differentiation, and cardiovascular defects (Regan et al., 2002; Sohn et al., 2002;

Wang X. et al., 2005). ERK5 is required for muscle cell differentiation, the survival of endothelial cells and the development of the immune cells in adults (Rovida et al., 2008; Dinev et al., 2001; Pi et al., 2004; Roberts et al., 2010; Sohn et al., 2008). It also mediates the G1/S transition of hepatocytes in liver regeneration and cell cycle progression from the G2 phase to mitosis, and promotes cell survival (Li Z. et al., 2012). Recently, the role of ERK5 in the epithelial-mesenchymal transition has been described. This process involves the transdifferentiation of epithelial cells, where they lose their cuboidal morphology and polarity and acquire a fibroblastoid phenotype with migratory capabilities under certain conditions and specific factors (Zavadil et al., 2005). ERK5 has been implicated in the transcriptional and post-translational regulation of EMT master proteins Slug and Snail (Arnoux V et al., 2008; Marchetti et al., 2008).

In agreement with its involvement in deregulated cellular functions in tumors, ERK5 signaling pathway is constitutively active in many human cancers, following activation by different oncogenes or by gene amplification, where it contributes to the acquisition of a more malignant and metastatic phenotype, resistance to apoptosis, angiogenesis, drug resistance.

Furthermore, its deregulation correlates with a poor prognosis (Esparís-Ogando et al., 2002; Mehta et al. 2003; Ramsay et al. 2011; Simões et al. 2015; Weldon et al. 2002; Zen et al. 2009).

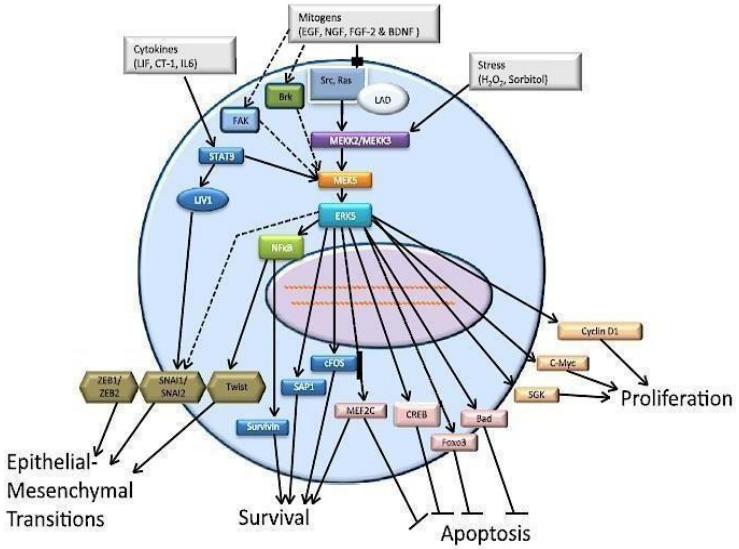

Figure 8. *Cellular processes involving ERK5*

2.2 Pharmacological inhibitors of ERK5

The large body of evidence of a role of ERK5 in cancer makes it a promising target for cancer therapy. Preclinical data have confirmed that inhibition of ERK5 activity effectively suppresses tumor growth (Yang et al., 2011). Several specific MEK5/ERK5 pathway pharmacological inhibitors have recently been developed. These include BIX02188, and BIX02189, which selectively inhibit MEK5 and to a lesser extent ERK5 activity (Tatake et al. 2008). However, as described above, ERK5 can be phosphorylated and activated in an MEK5-independent manner during mitosis, since the two drugs appear ineffective in inhibiting ERK5 signaling in highly proliferative tumor lines. Another widely used inhibitor of ERK5 activity is XMD8-92 (Rovida et al., 2015). Preclinical studies in mice have shown high tolerability to this compound and no side effects. In addition, the antitumor effect was effective: the inhibitor blocked ERK5 activity *in vivo*, reducing tumor growth and tumor-associated angiogenesis by 95% (Yang et al., 2010). Professor Marra's group demonstrated the drug's efficacy in reducing tumor mass and inhibiting its metastatic capacity in preclinical studies on hepatocellular carcinoma (Rovida et al., 2015).

Administration of XMD8-92 has also shown efficacy in ductal adenocarcinoma and neuroblastoma, in reducing significantly tumor cell growth *in vitro* and *in vivo* (Stecca et al., 2019; Sureban et al., 2014). Although XMD8-92 has been widely used as a highly specific ERK5 inhibitor, off-target activity against the BET bromodomain family member BRD4 has been recently described (Howell SJ et al., 2021).

Long non-coding RNA (lncRNA)

Although about 80% of the genome is transcribed into RNA, less than 2% is translated into functional proteins. It suggests that the primary function of the transcriptome is to produce non-coding RNA, including long non-coding RNA (lncRNA). While small RNAs are increasingly well-characterized, the role of lncRNAs, particularly in cancer, remains to be deeper investigated and understood.

LncRNAs can be categorized into different types based on their position on the genome, including intronic or exonic sense-overlapping lncRNAs, intergenic lncRNAs, antisense lncRNAs, bidirectional lncRNAs, and enhancer lncRNAs. It is important to note that this categorization is based on the location of the

lncRNAs on the genome (Esteller et al., 2011; Thum & Condorelli, 2015). Thus, the function of long non-coding RNAs (lncRNAs) depends on their subcellular localization (Chen L et al. 2016).

In most cases, lncRNAs are exclusively localized in the nucleus (30%), playing a crucial role as transcriptional and epigenetic modulators. A minority of lncRNAs are localized solely in the cytoplasm (15%), functioning as mRNA stability and translation regulators (Kapranov et al., 2007; Mercer & Mattick, 2013).

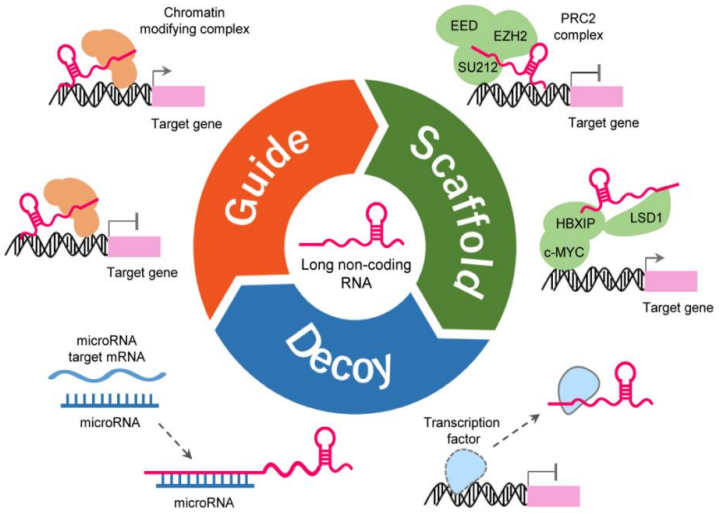

Figure 9. *lncRNA functions and mechanism of action (Dong et al., 2018)*

One of the primary characteristics of lncRNAs is their ability to form secondary or tertiary structures, which can bind to other molecules, including DNA, RNA, and proteins, and regulate gene expression (Liu et al., 2017). Specific long non-coding RNAs (e.g. HOTAIR or MALAT1) can act as scaffolds for chromatin remodeling complexes, responsible for repressive or activating marks deposition to particular chromatin sites. For instance, they can recruit polycomb repressive complex 1 or 2 (PRC1 or PRC2) to silence specific genes, or conversely, they can recruit HBXIP and LSD1 to activate the transcription of genes, such as c-MYC (Mercer et al., 2009; Tripathi et al., 2010; Kotake et al., 2011; Wang & Chang, 2011; Li Y. et al., 2016; Xie et al., 2016). Notably, lncRNAs can be recruited to specific genomic loci by means of their interaction with transcriptional factors, thus forming tripartite complexes with them and chromatin modifiers. This function, in particular, has been ascribed to HOTAIR, and found causative to EMT induction by the transcriptional factor Snail (Battistelli C et al., 2017).

In addition, lncRNAs can function to sequester transcription factors, thereby repressing the expression of their target genes. They can also act as molecular sponges, sequestering miRNAs and impair their binding to target mRNAs (Mercer et al., 2009;

Tripathi et al., 2010; Kotake et al., 2011; Wang & Chang, 2011; Li Y. et al., 2016; Xie et al., 2016).

Specific long non-coding RNAs (lncRNAs) can regulate RNA splicing by interacting with splicing factors or binding to the splicing junctions in pre-mRNA (Mercer et al., 2009; Tripathi et al., 2010; Kotake et al., 2011; Wang & Chang, 2011; Li Y. et al., 2016; Xie et al., 2016).

Research indicates that lncRNAs play a significant role in tumor processes, with some being up-regulated or down-regulated (Prensner & Chinnaiyan, 2011; Wang Y. et al., 2016).

While some lncRNAs are expressed in a cell-specific manner during cell differentiation, they are also expressed during tumor progression (Schmitt & Chang, 2016).

Dysregulation of lncRNAs is associated with tumorigenesis, tumor progression, metastasis, and poor prognosis, indicating that they may serve as biomarkers for cancer (Shi et al., 2016).

Through the mechanisms discussed above, long non-coding RNAs regulate pathways involving all cancer hallmarks, exerting their role as either oncogenes or suppressors (Prensner & Chinnaiyan, 2011; Schmitt & Chang, 2016; Wang Y. et al., 2016).

Due to their mechanistic and functional involvement in tumor

processes, lncRNAs have been explored as potential therapeutic targets.

3.1 MALAT1

The lncRNA MALAT1, Metastasis-associated lung adenocarcinoma transcript 1, also known as nuclear enriched abundant transcript 2 (NEAT2), is located on chromosome 11q13 and, once transcribed, is mainly localized in the nucleus (Zhang X et al., 2017).

The primary transcript of MALAT is 8kb; later, RNase P and RNase Z act to create a larger fragment of about 6.7 kb and a smaller fragment of 61 nucleotides (Wilusz J.E. et al., 2008). The larger fragment is very stable; in tumors, it has up to 12 h half-life, having a unique triple helix structure at 3' that protects it from exonucleases (Brown J.A. et al., 2014; Tani H et al., 2010). In addition, further stability is provided by the antisense TALAM1, which maintains high levels of MALAT1 through a positive regulatory loop (Zong X et al., 2016). The larger fragment, once mature, localizes in nuclear speckles, mainly in areas with active chromatin and colocalizing with the lncRNA NEAT1 (Wilusz J. E. et al., 2008; West J. A. et al., 2014). The short

fragment has structural similarities with tRNAs and is mainly localized in the cytoplasm, and its function is currently unknown (Wilusz J. E. et al., 2008).

MALAT1 is involved in the transcription and post-transcriptional regulation of genes. It acts as a cis/trans element or recruiting proteins to nuclear speckles (NSs), particularly those in the polycomb repressive complex family (Sun Q et al., 2018; Fan Y et al., 2014).

Under stress conditions, MALAT1 regulates HIF2a, ER/Enos, and CREB (Sun Q et al., 2018).

MALAT1 regulates alternative splicing and pre-mRNA splicing by interacting with trans-acting factors, such as serine/arginine-rich nuclear phosphoproteins (SR proteins) in NSs. Dephosphorylation of SR proteins modulates the splicing of many pre-mRNAs and the export of mRNAs from the nucleus. MALAT1 knockdown leads to this process. (Tripathi V et al. 2010). MALAT1 also interacts with RNA binding proteins (RBPs) (Scherer M et al., 2020).

MALAT1 knockdown does not have a phenotypic effect on mice at the physiological level, maybe because MALAT1 is particularly active under cellular stress rather than physiological conditions (EiSmann M et al., 2012).

It regulates gene expression as a molecular sponge for miRNAs, affecting cell proliferation and metastasis (Li Z-X et al., 2018).

In retinoblastoma, MALAT1 regulates cell proliferation by upregulating Wnt/β-catenin signaling and the MAPK/ERK pathway through inhibition of miR-124 (Liu S et al., 2018).

A previous study showed that MALAT1/miR-146a crosstalk can upregulate PI3K/AKT/mTOR in hepatocellular carcinoma (HCC) cell lines (Peng N et al., 2020).

In pancreatic cancer, there was an increased MALAT1 expression leading to YAP1 upregulation; instead, silencing MALAT1 reversed this effect, reducing pancreatic tumor size and volume in a xenograft mouse model (Zhou Y et al., 2018).

In NSCLC, the knockdown of MALAT1 by miR-101-3p inhibited growth and metastasis by downregulating the PI3K/AKT pathway (Zhang X et al., 2017).

MALAT1 promotes metastasis by regulating epithelial-mesenchymal transition and angiogenesis. In a preclinical study on cervical cancer cell lines, MALAT1 induced EMT, which increased invasion and metastasis. Conversely, silencing MALAT1 reduced EMT by downregulating mesenchymal markers such as MMP, cadherin, and vimentin (Sun R et al., 2016). ChIP-seq analysis showed that YAP1 induces MALAT1

expression, promoting angiogenesis factors such as VEGF, TWIST, and SLUG proteins by suppressing miR-126-5p in CRC (Sun Z et al., 2019). In NSCLC, ER-β binds to the estrogen response element of MALAT1, promoting the formation of vasculogenic mimicry (VM) by sponging off miR-145-5p, thereby inducing the expression of NEDD9, which, in turn, promotes EMT and metastasis (Yu W et al., 2019).

Cancer cells are subjected to various stresses, such as hypoxia, DNA damage, excessive signaling, and matrix detachment. Cells respond to these stresses through apoptosis, DNA repair, inflammation, and autophagy (Fouad Y.A. et al., 2017). Various preclinical studies have shown that MALAT1 regulates these pathways. Inflammatory cytokines, such as interleukin (IL)-6, IL-8, and TGF-β, regulate MALAT1 transcription via the STAT3 pathway (Hao Y. et al., 2020; Zheng T. et al., 2019; Wang Y. et al., 2018). MALAT1 can also regulate NFκB in childhood hemangioma. In a xenografted hemangioma mouse model, silencing of MALAT1 inhibited tumor growth via miR-424 (Li M-M et al., 2019).

Although MALAT1 is primarily known as an oncogene and is upregulated in most cancer types, some studies suggest it may also have tumor suppressor functions. For instance, in lung

cancer, breast cancer, glioma, and endometrial cancer, downregulated expression of MALAT1 has been linked to proliferation and metastasis (Guo F. et al., 2015; Kim J. et al., 2018; Cao S. et al. 2016; Li Q. et al., 2016). Reduced expression of MALAT1 in breast cancer tissue is associated with high-grade metastasis (Kim J. et al., 2018). MALAT1 also exerts its tumor suppressor function by inhibiting EpCAM and ITGB4, potent pro-invasive genes, as shown in a study on breast and colon cancer tissue. Additionally, PTEN, a tumor suppressor, modulates the action of MALAT1 by onco-miR sponging (Kwok Z.H. et al.,2018).

A study showed that the MALAT1/HuR complex suppresses the CD133 gene, decreasing EMT in triple-negative breast cancer (Latorre E. et al., 2016).

MALAT1 acted as a tumor suppressor in glioma patients by deactivating the ERK/MAPK pathway through miR-155 downregulation and FBXW7 activation. This is in accord with the improved survival of patients with reduced MALAT1 expression (Cao S. et al., 2016).

AIM OF THE WORK

The transcriptional cofactor Yes-Associated Protein (YAP) is known to be a master regulator of gene expression able to induce cellular reprogramming towards different cellular states. There is increasing evidence that the composition and genomic occupancy of YAP-recruiting transcriptional complexes may depend on tissue and cellular context, thereby driving specific gene expression and different functional outcomes. Furthermore, the formation of these complexes may be regulated by the phosphorylation status of the components, which depends on the activity of enzymes belonging to different signaling pathways. Therefore, it is critical to understand better how the activity of complexes that include YAP may be controlled by studying new members and functional roles.

Based on our recent work (to which I contributed as co-first author; see Ippolito and Consalvi et al., 2023) identifying STAT3 as a new interactor of YAP in liver cells and ERK5 as a new regulator of YAP activity, and on recent literature data showing lncRNAs as functional components of transcriptional molecular platforms, my PhD project aimed to the structural and functional characterization of YAP-enrolled transcriptional complexes and of their regulation by ERK5/MAPK.

To pursue these goals, I have i) investigated the role of STAT3 in the YAP-dependent gene expression, ii) analyzed the mechanistic and functional role of ERK5 in the control of the assembly/activity of YAP/STAT3 and YAP/TEAD complexes and of their recruitment on DNA, and iii) evaluated lncRNAs as potential members of the YAP-dependent molecular platforms and their functional role in YAP-driven cellular outcomes.

Overall, data obtained in this study provided new knowledge of how specific partners of YAP in transcriptional complexes and signaling pathways regulating the complex formation/activity can drive specific YAP-dependent gene expression and specific YAP-induced cell outcomes in liver cells. In perspective, these studies may pave the way to new translational approaches aimed at interfering with YAP activity in pathologies where it has been found deregulated.

MATERIAL AND METHODS

Cell cultures and treatments

The human HuH7 liver carcinoma cells were grown in Dulbecco's modified Eagle's medium (DMEM; Gibco-Life Technologies), supplemented with 10% fetal bovine serum (FBS), 2mM glutamine (Gibco-Life Technologies), and antibiotics (Gibco-Life Technologies) at 37°C in a humidified atmosphere with 5% CO2 on plastic (Corning).

Resident liver stem cells (RLSCs), HepE14 and HepD3 hepatocytes are immortalized, and non-tumorigenic cell lines derived from murine liver explants at 14th day of development or at 3 days post-birth (Amicone L et al. 1997; Conigliaro A et al. 2008). RLSCs exhibit a typical stem cell gene profile, self-renewal capacity, and multilineage differentiation potential. Hepatocyte cell lines exhibit a differentiated phenotype and a consistent gene expression profile. RLSC and hepatocytes were grown as previously described (Noce et al., 2019).

Where indicated, cells were treated with 10μM or 20 μM MEK5/ERK5 inhibitor BIX02189 (Selleckchem, Selleck Chemicals GmbH), 10μM of YAP-TEAD interaction inhibitor

Verteporfin (PeproTech Inc., Rocky Hill, NJ, USA), 5μM of STAT3 inhibitor Stattic (Selleckchem, Selleck Chemicals GmbH) for the specified time, 1 μg/ml of Nocodazole (Sigma-Aldrich).

Cell transfections

YAP-overexpressing cells were obtained by transient transfection with pQCXIH-Myc-YAP or pQCXIH-Myc-YAP5SA (gift from Kunliang Guan, Addgene plasmids # 33091 and # 33093) (Zhao B et al. 2007), or with Flag-YAP or Flag-YAP5SA (Addgene), respectively, using Lipofectamine™ LTX Reagent with PLUS™ Reagent (Thermo Fisher Scientific) or Lipofectamine 3000 (Thermo Fisher Scientific) according to the manufacturer's protocol. Cells were collected 48 hours after transfection or utilized for treatments. Notably, the YAP5SA protein, carrying mutations of LATS1/2-dependent phosphorylation sites (S61A, S109A, S127A, S164A, S381A), results constitutively active (Zhao B et al. 2007).

ERK5-overexpressing cells were obtained by transient transfection with pCMV-ERK5 (carrying the human ERK5 cDNA, kindly provided by J.E. Dixon). Control cell lines were obtained by transfection with the empty vector. According to the

manufacturer's protocol, cells were transfected with Lipofectamine™ LTX Reagent with PLUS™ Reagent (Thermo Fisher Scientific) or Lipofectamine 3000 (Thermo Fisher Scientific) and collected 48 h after transfection.

STAT3-overexpressing cells were obtained by transient transfection with Stat3 Flag pRc/CMV (Addgene, Plasmid #8707), respectively, using Lipofectamine™ LTX Reagent with PLUS™ Reagent (Thermo Fisher Scientific) or Lipofectamine 3000 (Thermo Fisher Scientific) according to the manufacturer's protocol. Cells were collected 48 hours after transfection or utilized for treatments.

3D Cell cultures and analysis

For the 3D cell culture experiments, YAP-overexpressing HuH7 cells were obtained by transient transfection with pQCXIH-Myc-YAP or the empty vector as control. Then, 24h after transfection, cells were seeded on a low attachment substrate (0.6% agar) until suspended aggregates/spheroids formed (24 h). Moreover, 48 h after transfection, spheroids were treated with 5μM of STAT3 inhibitor, Stattic (Selleckchem, Selleck Chemicals GmbH) or DMSO for 24h.

Spheroid cultures were analyzed using OrganoSeg (Borten, M.A et al., 2018). Spheroids' images were uploaded to the software and then segmented, which means that the program apports some corrections to the images to analyze them as well as possible. First of all, it has been made the out-of-focus correction (default ON) to include blurred content outside of the image plane, or the DIC correction (default OFF), for a tighter identification of the spheroid's border. Other segmentation parameters have been adjusted:

- intensity threshold slider (0,96) to identify higher contrast differences.
- window size slider (250), larger window sizes capture a more global detail; smaller window sizes capture a more local detail. Ideal window size varies from image to image.
- size threshold (160) to eliminate organoids under the specified pixel area value, thus excluding single cells from the analysis.

The user may select as many of the metrics to export as preferred. We analyzed the number of spheroids, contrast, energy, and homogeneity.

Bioinformatic analysis of ChIP-seq datasets

Two previously published datasets were analyzed for ChIP-seq analysis on hepatocytes. The first dataset was a ChIP-seq of YAP, which identified many TEAD binding sites for which YAP made contact only when activated by Myc (Croci O et al., 2017). The second dataset was a ChIP-seq for STAT3, which identified STAT3 binding sites on genes upon activation by IL6 (Goldstein I et al., 2017). The datasets were aligned to the latest version of the murine genome, mm10, using Bowtie2. The obtained data were analyzed with Macs2, using the gene promoter as a parameter. The gene promoter was defined as the 2000 nt region upstream and 1000 nt downstream of the TSS. This analysis identified 497 promoters bound by STAT3, 10514 by YAP (with Myc activated), and 415 by both. YAP, STAT3 and TEAD peak overlap in 413 gene promoters.

For the analysis of ChIP-seq on triple-negative breast cancer cells, two datasets were examined: a ChIP-seq of YAP in MDA-MB-231 (Zanconato F et al., 2015) and a ChIP-seq of STAT3 in MDA-MB-231 (McDaniel JM et al., 2017). The datasets were aligned to the most recent version of the human genome, GRCh38, using Bowtie2, and the obtained data were analyzed

with Macs2. Peaks were selected by placing a threshold of 2-fold enrichment in consensus sequence frequency compared to baseline (YAP 0.2 and STAT3 0.1). The peaks within 20000 base pairs of the TSS were selected. This analysis revealed that the peaks of YAP and STAT3 are located within 500nt of each other and also showed an overlap of the peaks of YAP, STAT3, and TEAD, identifying 254 candidate genes.

Subsequently, GO term (Gene Ontology) analysis was performed for both analyses.

RNA interference

RNA interference (RNAi) was used to silence STAT3 genes using either chemically synthesized double-stranded small interfering RNA (siRNA) cells were transfected with equal amounts (100 pmol) of ON-TARGET SMARTpool human STAT3 (Merck EHU122051) siRNAs using Lipofectamine RNAiMAX (Thermo Fisher Scientific) reagent in OptiMEM following the manufacturer's protocol. RNA and proteins were harvested and analyzed after 16 or 36h. Negative controls included siRNA against GFP (Gene Pharma).

Luciferase assays

To analyze endogenous ERK5 and YAP activity, cells were plated in 60 mm plates and co-transfected by Lipofectamine™ LTX with PLUS™ Reagent or Lipofectamine™3000 (Thermo Fisher Scientific) according to the manufacturer's protocol with the following construct: MEF2-luc reporter (Woronicz JD et al., 1995), 8XGTIIC-luc reporter (gift from Stefano Piccolo; Addgene plasmid # 34615) (Dupont S et al. 2011) (1 μg), Renilla expression vector (0.2 μg), pcDNA3 empty vector (4 μg). After 24 h, cells were moved into 12-well plates and treated in triplicate with Nocodazole for further 24h. All treatments were performed in triplicate.

Luciferase activity was measured using the Dual-Luciferase Reporter Assay System kit (Promega Corporation, Madison, WI) according to the manufacturer's instructions and normalized for Renilla Luciferase activity.

RNA isolation and quantitative RT-PCR

Total RNAs were extracted with ReliaPrep™ RNA Miniprep Systems (Promega) according to the manufacturer's protocol and reverse-transcribed using Biorad iSCRIPT cDNA Synthesis Kit (BioRad). cDNA was amplified by qPCR using GoTaq qPCR Master Mix (Promega Corporation, Madison, WI) in BioRad-iQ-iCycler. Relative amounts, calculated with the 2(−ΔCt) method, were normalized concerning the housekeeping gene RPL34 (60 S ribosomal protein L34). The sequence of murine and human primers utilized are listed in Table 1 and Table 2, respectively.

Gene	Sequences
Rpl34	For: 5′- GGAGCCCCATCCAGACTC-3′ Rev: 5′- CGCTGGATATGGCTTTCCTAT-3′
Malat1	For: 5′- CCAATTACCTCCCCTACACA-3′ Rev: 5′-ACCTCCCAGTTTTGTAAGAC -3′

Table 1. *RT-qPCR mouse oligonucleotides*

Gene	Sequences
Ctgf	For: 5′- AGGAGTGGGTGTGTGACGA-3′ Rev: 5′- CCAGGCAGTTGGCTCTAATCA-3′
Cyr61	For: 5′- AAGAAACCCGGATTTGTGAG-3′ Rev: 5′- GCTGCATTTCTTGCCCTTT-3′
Ankrd1	For: 5′- AGTAGAGGAACTGGTCACTGG-3′ Rev: 5′- TGGGCTAGAAGTGTCTTCAGAT-3′
Erk5	For: 5′- CTGTCTACGTGGTCCTGGAC-3′ Rev: 5′- GCCTTGTCCAAGTCCAAGTC-3′
Yap	For: 5′- GTCCCGAACCCCTGGTAATAG-3′ Rev: 5′- GGCCCTGCTGACATGTTTCTT-3′
Rpl34	For: 5′- GGAGCCCCATCCAGACTC-3′ Rev: 5′- CGCTGGATATGGCTTTCCTAT-3′
Malat1	For: 5′-AGCCCAAATCTCAAGCGGTGC -3′ Rev: 5′- TGCATCGAGGTGAGGGGTGA-3′

Table 2. *RT-qPCR human oligonucleotides*

SDS-PAGE and Western Blotting

For protein extraction, cells were washed twice in PBS1X and lysed on ice directly on the plate with RIPA buffer (50 mM Tris-HCl pH 7.6, 150 mM NaCl, 0.5% sodium deoxycholate, 0. 1% SDS, 1% NP40) containing protease inhibitors (complete, EDTA-free protease inhibitor cocktail; Sigma-Aldrich) and phosphatase inhibitors (5 mM EGTA pH 8.0; 50 mM sodium fluoride; 5 mM sodium orthovanadate).

Samples (20 μg protein) prepared in a Laemmli buffer solution (containing 2-β-mercaptoethanol and SDS) were boiled at 95°C for 10 minutes and loaded onto 8% polyacrylamide gels (for ERK5 phosphorylation analysis) or 12% gels, which were then transferred to a nitrocellulose membrane (Pure Nitrocellulose Membrane 0. 45 μm; Bio-Rad) at 15V for 50 minutes in a transfer buffer (50 mM Tris, 40 mM glycine, 0.1% SDS, 20% methanol).

They were then incubated overnight at four °C with one of the following primary antibodies: rabbit monoclonal anti-ERK5 antibody (#3372, Cell Signaling, diluted 1:10000); monoclonal anti-tubulin antibody (B-7, sc-5286, Santa Cruz, Biotechnology, diluted 1: 1000); anti-STAT3 monoclonal antibody (124H6, Cell Signaling 9139S, diluted 1:1000); mouse anti-GAPDH

monoclonal antibody (Millipore, diluted 1:1000); mouse anti-YAP monoclonal antibody (SC-101199. Santa Cruz Biotechnology diluted 1:1000).

After three 10-minute washes with 1X PBS-T, the filters were incubated with a species-specific secondary antibody, mouse anti-IgG (diluted 1:5000) or rabbit anti-IgG (diluted 1:5000) conjugated with peroxidase enzyme (Bio-Rad, Hercules, CA, USA) for 1 hour in a shaking condition.

Chemiluminescence detection was performed using a specific ECL kit (ECL, Bio-Rad Laboratories Inc., Hercules, CA, USA).

WB on PhosTag gel

For protein extraction, cells were washed twice in PBS1X and lysed on ice directly on the plate with RIPA buffer (50 mM Tris-HCl pH 7.6, 150 mM NaCl, 0.5% sodium deoxycholate, 0. 1% SDS, 1% NP40) containing protease inhibitors (complete, EDTA-free protease inhibitor cocktail; Sigma-Aldrich) and phosphatase inhibitors (50 mM sodium fluoride).

Samples (20 μg protein) were precipitated with TCA (Trichloroacetic acid) and then prepared in a Laemmli buffer solution (containing 2-β-mercaptoethanol and SDS) were boiled at 95°C for 10 minutes and loaded onto Phostag gels

(SuperSepTM Phos-tagTM (50umol/l), 7.5%, 17well, 83×100×3.9mm, 5 Gels, Fujifilm). After transfer, the gel was washed with a transfer solution added with EDTA to chelate Mg2+ ions and ensure correct passage of current during transfer. Then, gels were transferred to a nitrocellulose membrane (Pure Nitrocellulose Membrane 0. 45 μm; Bio-Rad) at 15V for 50 minutes in a transfer buffer (50 mM Tris, 40 mM glycine, 0.1% SDS, 10% methanol).

They were then incubated overnight at four °C with one of the following primary antibodies: rabbit monoclonal anti-ERK5 antibody (#3372, Cell Signaling, diluted 1:10000); anti-STAT3 monoclonal antibody (124H6, Cell Signaling 9139S, diluted 1:1000); mouse anti-YAP monoclonal antibody (SC-101199. Santa Cruz Biotechnology diluted 1:1000); mouse polyclonal α-TEAD4 (ab58310, Abcam, 1:500).

After three 10-minute washes with 1X TBS-T, the filters were incubated with a species-specific secondary antibody, mouse anti-IgG (diluted 1:5000) or rabbit anti-IgG (diluted 1:5000) conjugated with peroxidase enzyme (Bio-Rad, Hercules, CA, USA) for 1 hour in a shaking condition.

Chemiluminescence detection was performed using a specific ECL kit (ECL, Bio-Rad Laboratories Inc., Hercules, CA, USA).

Chromatin Immunoprecipitation (CHIP)

For chromatin immunoprecipitation (ChIP) we used two different approaches.

For endogenous protein immunoprecipitation we used 5 μg of the following antibodies were used: rabbit polyclonal α-YAP (H-125X, Santa Cruz Biotechnology Inc.), rabbit monoclonal α-YAP (D8H1X, 14074, Cell Signaling), mouse α-STAT3 (124H6, Cell Signaling), mouse polyclonal α-TEAD4 (ab58310, Abcam, 1:500), or the negative control rabbit IgG (Millipore Corp., Bedford, MA, USA) mouse IgG (Millipore Corp., Bedford, MA, USA).

For exogenously overexpressed protein immunoprecipitation, cells were transfected with pQCXIH-Myc-YAP, pCMV-ERK5-HA or Stat3 Flag pRc/CMV or the respectively empty vectors, and we immunoprecipitated with Anti-C-Myc Magnetic Beads (SAE0201-1ML Merck), Ezview Red anti-HA Affinity Gel (E6779-1ML Merck) or Anti-Flag (R) M2 magnetic beads (M8823-1ML Merck).

Equal amounts of immunoprecipitated DNA and relative controls were used for qPCR analysis, performed in triplicate. The primers used are listed in Table 3. The promoter of RPL30

was used as a negative control. qPCR analysis of immunoprecipitated samples (IP) and negative controls (IgG or CTRL) were both normalized to total chromatin input and expressed as (IP/IgG)/input or (IP/CTRL)/input.

Promoter	Sequences
pSNAIL (STAT3 binding site)	For: 5′- TGT TCA GGG CTG TGT AGA C-3′ Rev: 5′- GAG CTG CTG ACC TTT GG-3′
pCTGF (TEAD binding site)	For: 5′- CAA TCC GGT GTG AGT TGA TG -3′ Rev: 5′- GGC GCT GGC TTT TAT ACG -3′
pRPL30	For: 5′-TAAGGCAGGAAGATGGTGG -3′ Rev: 5′-CAGTGTGCTCAAATCTATCC -3′

Table 3. *qPCR oligonucleotides*

RNA immunoprecipitation (RIP)

In UV cross-linking RIP, cells were washed twice with PBS and subjected to UV cross-linking (one-time irradiation at 800 mJ/cm2 in 254 nm Stratalinker (Stratagene 2400, Stratagene). Cells were then lysed in 10 mM HEPES (pH 7.3), 20 mM KCl, 2

mM MgCl2, 0.5 mM EGTA, 1 mM EDTA, 1 mM DTT, 40 U/mL RNAsin inhibitor, 0.1% SDS, 0.5% sodium deoxycholate, and 0.5% NP40. Exogenous YAP was immunoprecipitated with AntiFlag(R) M2 magnetic beads (M8823-1ML Merck) and incubated for 2 hr. Denaturing washes were performed as described previously (Battistelli et al., 2017). Coimmunoprecipitated lncRNAs were extracted using Qiazol and the miRNeasy kit (Qiagen).

qPCR analysis was performed with GoTaq qPCR Master Mix (Promega Corporation, Madison, WI) in BioRad-iQ-iCycler, and lncRNA fold enrichment in immunoprecipitated samples was expressed as percent input and compared to the control normalizing on the control RNA RPL34.

Gene	**Sequences**
MALAT1	For: 5′-AGCCCAAATCTCAAGCGGTGC -3′ Rev: 5′- TGCATCGAGGTGAGGGGTGA-3′
RPL34	For: 5′- GGAGCCCCATCCAGACTC-3′ Rev: 5′- CGCTGGATATGGCTTTCCTAT-3′

Table 4. *RT-qPCR oligonucleotides in RIP experiments*

Co-immunoprecipitation assays

HuH7 cells were transfected by Lipofectamine 3000 (Invitrogen) with the indicated plasmids and treated with BIX02189 or DMSO at 24 h post-transfection. Cells were harvested 16 h after treatments and lysed in Triton 1X lysis buffer (150 mM NaCl, 50 mM Tris–HCl pH 7.5, 2 mM EDTA, 1% Triton-X100, 10% glycerol) supplemented with protease and phosphatase inhibitors.

For protein immunoprecipitation, protein extracts from cells overexpressing the target protein or control cells (1 mg) were incubated with 30 µl of beads Anti-C-Myc Magnetic Beads (SAE0201-1ML Merck), Ezview Red Anti-HA Affinity gel (E6779-1ML Merck) or Anti-Flag(R) M2 Magnetic Beads (M8823-1ML Merck) at 4 °C for 1h. Then, the beads were washed four times with a Triton 1X lysis buffer. The immune complexes were eluted and denatured with Laemmli buffer 1X. Total and immunoprecipitated proteins were resolved on SDS-PAGE and transferred to the nitrocellulose membrane. For immunoblotting, the following primary antibodies were used: mouse polyclonal α-YAP (SC-101199, Santa Cruz Biotechnology, inc.; 1:1000), mouse polyclonal α-TEAD4

(ab58310, Abcam, 1:500), rabbit monoclonal anti-ERK5 antibody (#3372, Cell Signaling, diluted 1:10000); anti-STAT3 monoclonal antibody (124H6, Cell Signaling 9139S, diluted 1:1000); mouse monoclonal α-tubulin (B-7, sc-5286, Santa Cruz Biotechnology, 1:1000), anti-GAPDH monoclonal antibody (Millipore, diluted 1:1000). Blots were then incubated with HRP-conjugated species-specific secondary antibodies (Bio-Rad, Hercules, CA, USA) or Goat α-mouse IgG light-chain specific antibody (HPR conjugate, #91196, Cell Signaling Technology), followed by Enhanced Chemiluminescence reaction (ECL, Bio-Rad Laboratories Inc., Hercules, CA, USA).

In vitro translation (IVT)

In vitro-translated (IVT) proteins were produced with the TNT Coupled Reticulocyte Lysate Systems Kit (Promega). According to the manufacturer's instructions, the following reaction was assembled:

- TNT Rabbit Reticulocyte Lysate 25µl;
- TNT Reaction Buffer 2µl;
- T7 TNT RNA Polymerase 1µl;
- Amino Acid Mixture, Minus Leucine, 1ul;

- Amino Acid Mixture, Minus Methionine, 1ul;
- RNasin Ribonuclease Inhibitor (40u/µl) 1µl;
- DNA Template(s) (0.5µg/µl) 2µl;
- H2O to a final volume of 50µl.

The reaction was incubated for 30' at 90°C.

Kinase assays

For kinase assay, 5µl of IVT protein were incubated with 100 ng of recombinant ERK5 (ERK5 active; SignalChem), 1µl ATP 10mM (Cell signalling), and 23µl of Kinase Buffer 1X (SignalChem) at 30°C for 30'. When specified, 1µl of 10U/µL CIP (Calf Intestinal Phosphatase, New England BioLabs) was added for 1 hour at 37°C.

Where specified, the kinase assay has been carried out on immunoprecipitated proteins. In this case, HuH7 cells YAP-overexpressing were treated 24h after transfection with 10µM BIX02189 or DMSO. Lysates have been incubated for 1h at 4°C with Anti-Flag(R) M2 Magnetic Beads (M8823-1ML Merck).

The beads were then washed four times with Triton 1X lysis buffer and incubated with 100 ng of recombinant ERK5 (ERK5 active; SignalChem), 1µl ATP 10mM (Cell Signalling), and 23µl

of Kinase Buffer 1X (SignalChem) at 30°C for 30'. The immune complexes were eluted and denatured with Laemmli buffer 1X.

Statistical analysis

Statistical significance was determined by one-tailed paired or unpaired Student's t-test using GraphPad Prism Version 5 (GraphPad Software). A $p \leq 0.05$ was considered statistically significant (*$p < 0.05$; **$p < 0.01$; ***$p < 0.001$).

RESULTS AND DISCUSSION

1. STAT3 regulates YAP transcriptional and functional activity in hepatoma cells

Increasing evidence showed that YAP is recruited as a cofactor by several transcriptional factors besides, or in addition to, the well-known ones belonging to the TEAD family (Lopez-Hernandez A. et al., 2021). The variability of composition and genome occupancy of different transcriptional complexes, most likely dependent on different upstream regulations, could explain how YAP drives specific gene expression programs and controls several cell functions in a tissue- and cell-type-dependent manner.

Aiming to unveil and characterize YAP partners in controlling gene expression, we first focused on possible cooperation between this cofactor and STAT3. Our previous and published evidence in murine hepatocytes, indeed, demonstrated that the YAP-dependent expression of the EMT master gene Snail (whose promoter lacks TEAD consensus motifs within 1500 bp upstream) implies the YAP recruitment on a chromatin region including a STAT3 consensus (−350 from the TSS), where we

previously found STAT3 binding (Noce et al., 2019). Moreover, CoIP experiments demonstrated a physical interaction between these factors (Noce et al., 2019), which was coherent with what was observed in other cell types (Ying Shen et al., 2021).

Starting from these observations, we investigated in HuH7 hepatoma cells the role of STAT3 in the YAP-dependent gene expression. To this aim, we performed experiments of STAT3 functional impairment by pharmacological inhibition and genetic silencing in basal conditions or in overexpression of YAP. As shown in Figure 1A, while the treatment of HuH7 with the STAT3 inhibitor Stattic (a small molecule that selectively inhibits activation, dimerization, and nuclear translocation of STAT3) (Schust J et al., 2006) slightly impaired Snail transcription (that in these cells resulted already at low level; data not shown), it induced a significant transcriptional downregulation of CTGF and Cyr61, genes known until now to be mainly dependent on YAP/TEAD. The same result has been obtained by STAT3 knockdown by a siRNA-based approach (Figure 1C). Notably, in both experiments, a downregulation of YAP expression (both at RNA and protein level) has been also observed (Figure 1B and 1D), suggesting a transcriptional regulation of Yap gene by STAT3. However, the inhibition of

YAP-target gene expression following Stattic treatment can also be found in condition of YAP overexpression (where no change of YAP protein level can be observed) (Figure 1E and 1F), indicating that STAT3 regulates YAP transcriptional activity and suggesting a multilevel control by STAT3 on the YAP activity.

In accordance with transcriptional data, we found that STAT3 is required for YAP functional activity, assessed as the ability to promote, in hepatoma cells, tumor sphere formation in low attachment conditions. As shown in Figure 2, the overexpression of a constitutively active mutant of YAP (YAP5SA; Zhao B et al., 2007) in HuH7 cells affected both the number and the morphometry of 3D spheroids in terms of compactness, uniformity of the structure and homogeneity (sferic shape) evaluated by the use of OrganoSeg (a software able to quantify several parameters of spheroids and organoids) (Borten, M.A et al., 2018).

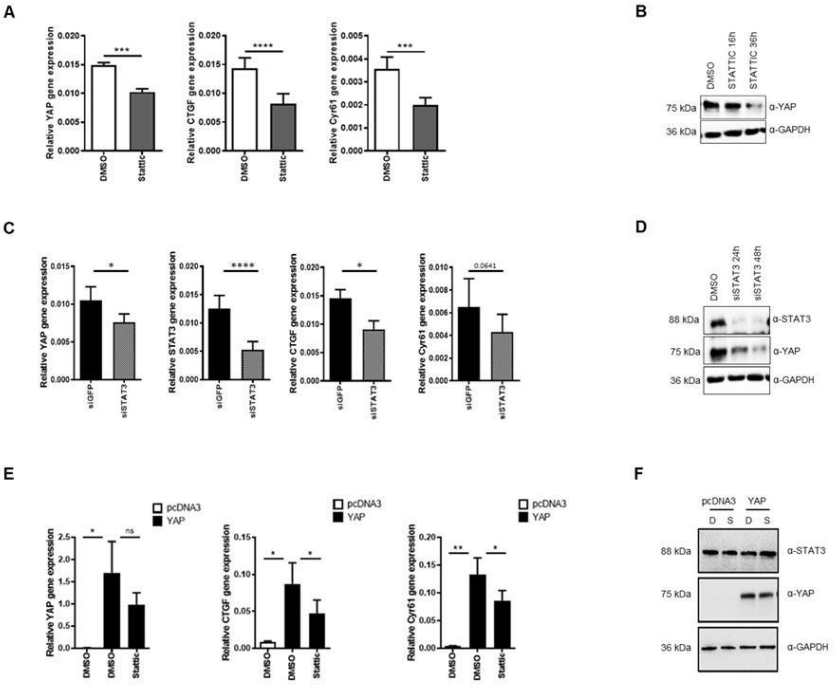

Figure 1

A. RT-qPCR analysis of the indicated genes in HuH7 treated with 5μM Stattic or DMSO. Data are expressed as relative gene expression and shown as mean ± S.E.M. of three independent experiments. Statistically significant differences are reported (***$p < 0.001$; ****$p < 0.0001$). **B.** Western blot for YAP protein in HuH7 treated with 5μM Stattic or DMSO for 16h or 36h. GAPDH has been utilized as a loading control. **C.** RT-qPCR analysis of the indicated genes in HuH7 transfected with siGFP or siSTAT3 siRNAs. Data are expressed as in (**A**). Statistically significant differences are reported (*$p < 0.05$; **$p < 0.01$; ***$p < 0.001$; ****$p < 0.0001$). **D.** Western blot for STAT3 and YAP in HuH7 treated with 5μM Stattic or DMSO for 16h or 36h. GAPDH has been utilized as a loading control. E. RT-qPCR analysis of the indicated YAP target genes in YAP-overexpressing HuH7 cells (YAP5SA)

and control cells (pcDNA3) treated with 5μM Stattic or DMSO. Data are expressed as relative gene expression and shown as mean ± S.E.M. of four independent experiments. Statistically significant differences are reported (*$p < 0.05$; **$p < 0.01$). **D.** Western blot for STAT3 and YAP in YAP-overexpressing HuH7 treated with 5μM Stattic or DMSO. GAPDH has been utilized as a loading control.

In particular, YAP overexpressing cells were able to form spheroids at a higher number, with a significant increase in the projected area (contrast) and minor compactness (energy) and homogeneity (homogeneity), all features coherent with the oncogenic activity of the protein. Notably, Stattic treatment significantly recovered all the YAP-triggered effects on spheroid morphometry and reduced their number (Figure 2).

Overall, the provided data indicate that STAT3 and YAP functionally interact in hepatoma cells to control gene expression and their 3D growth. Further studies will be needed to characterize the YAP-dependent functions involved in the observed changes and regulated by STAT3 activity.

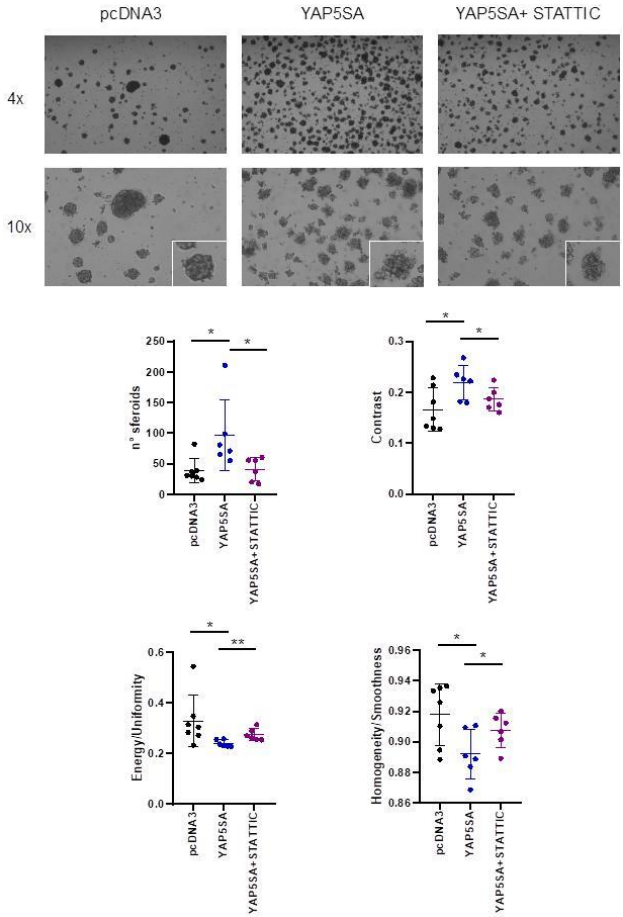

Figure 2. Representative images of spheroids in control (pcDNA3) or YAP-overexpressing HuH7 cells treated for 24 h with 5μM Stattic or DMSO. Data are reported as mean ± S.E.M. of six fields from two independent 3D cell cultures. Statistically significant differences are reported (unpaired, one-tailed Student's *t*-test; $*p < 0.05$; $**p < 0.01$). Bioinformatic analysis obtained by OrganoSeg software in the different cell conditions is shown.

Legend: Contrast, intensity contrast between pixel and neighbor (variance); Energy, the dominance of adjacent pixel combinations (uniformity); Homogeneity, the likelihood of adjacent pixels being equal (smoothness).

2. STAT3 cooperates with TEAD in the YAP-dependent target gene regulation

The involvement of STAT3 in the YAP-dependent CTGF and Cyr61 expression suggested the possibility of a transcriptional cooperation between STAT3 and YAP/TEAD. To enforce this hypothesis, we firstly performed an analysis of CTGF promoter by the Eukaryotic Promoter Database (EPD), which revealed consensus of both transcriptional factors close to each other. Moreover, a bioinformatic analysis on publicly available ChIP-seq datasets of STAT3, TEAD, and YAP from hepatocytes and triple-negative breast cancer cells (in collaboration with Prof. Valerio Fulci, Sapienza University of Rome) showed a large overlap between peaks of chromatin occupancy relative to all three factors on regulatory regions of various genes (Figure 3A and data not shown), whose GO terms are significantly enriched in biological processes related to tumor progression (i.e. cell locomotion, wound healing, chemotaxis, extracellular matrix remodeling, cell

migration) (Figure 3B), including CTGF (Figure 3C) (also involved in cell adhesion, chemotaxis, angiogenesis, matrix accumulation, and wound healing; Holbourn et al., 2008).

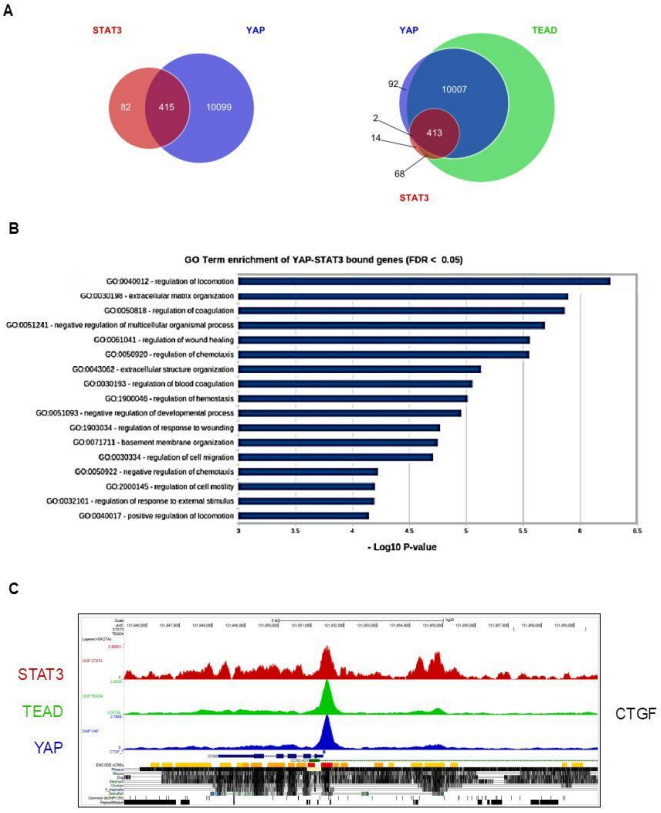

Figure 3.
A. ChIP-Seq Analysis in Hepatocytes (see M&M for the details)
B. Gene Ontology (GO) term enrichment analysis. Significantly enriched GO terms were selected based on an FDR < 0.05.

C. STAT3, TEAD, and YAP ChIP-Seq graph from Triple negative cancer cells showing the overlap of peaks on CTGF promoter

These elements, together with literature data indicating the possible regulation of YAP target genes by interaction in *cis* of TEAD and YAP with other TFs (i.e. AP1 and MRTF/SRF) (Zanconato et al., 2015; Liu et al., 2016) located on distant or proximal chromatin loci, prompted us to investigate the role of STAT3 (played alone or in a multimeric complex with TEAD), in the YAP-dependent gene expression.

Therefore, ChIP assays from hepatocyte cell lines overexpressing YAP have been performed and confirmed ChIP-seq data showing a significative binding of STAT3 and YAP both on Snail promoter (on chromatin fragments containing only the STAT3 consensus), as previously shown, and on CTGF promoter (on chromatin fragments including both STAT3 and TEAD consensus) (Figure 4A and 4B), where also TEAD was recruited (Figure 4C). Moreover, a transcriptional analysis of CTGF and Cyr61 from YAP overexpressing cells treated with Stattic and with the inhibitor of the interaction between YAP and TEAD, Verteporfin, alone or in combination, unveiled an equal contribution of the two TFs to the YAP-dependent CTGF and Cyr61 gene expression (Figure 4D).

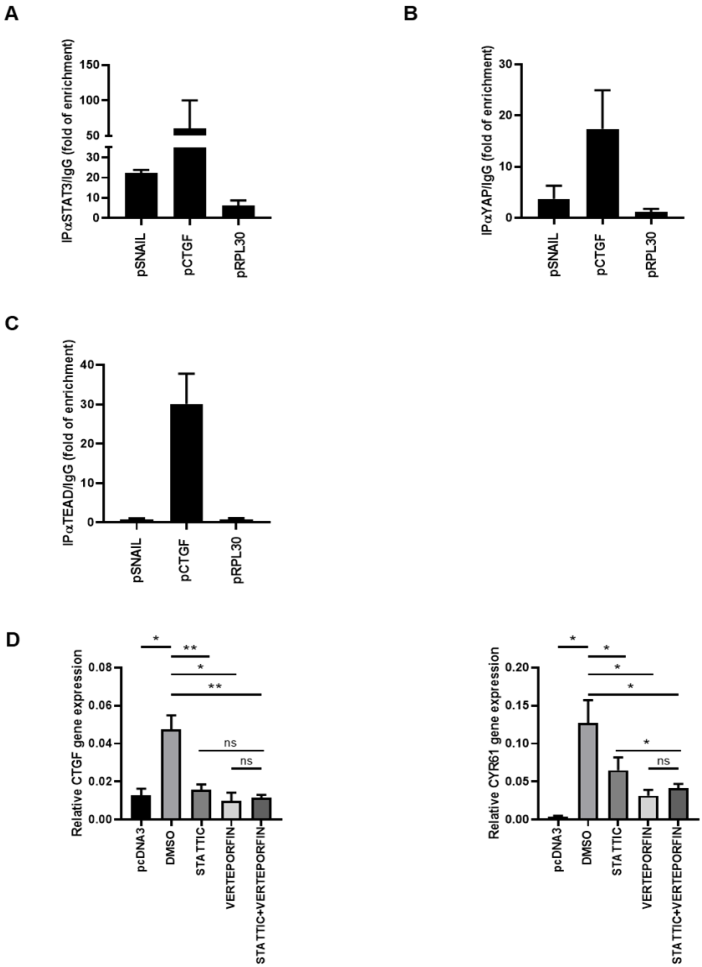

Figure 4

A qPCR analysis of ChIP assays with anti-STAT3 antibody (IP) and, as control, normal mouse IgG (IgG) on chromatin from YAP-overexpressing hepatocytes. The STAT3 consensus region embedded in the *Snail* gene promoter and the TEAD consensus region embedded in the *Ctgf* gene

promoter were analyzed. A STAT3 unbounded region of the *RPL30* promoter was utilized as a negative control. Data are normalized to total chromatin input and background (control immunoprecipitation with IgG) and expressed as fold of enrichment. Mean ± SEM of qPCR data obtained in duplicate from two independent experiments is reported. **B** qPCR analysis of ChIP assays with anti-YAP antibody (IP) and, as control, normal rabbit IgG (IgG) on chromatin from YAP-overexpressing hepatocytes. The STAT3 consensus region embedded in the *Snail* gene promoter and the TEAD consensus region embedded in the *Ctgf* gene promoter were analyzed. A YAP unbounded region of the *RPL30* promoter was utilized as a negative control. Data are normalized to total chromatin input and background (control immunoprecipitation with IgG) and expressed as fold of enrichment. Mean ± SEM of qPCR data obtained in triplicate from two independent experiments is reported. **C** qPCR analysis of ChIP assays with anti-TEAD antibody (IP) and, as control, normal mouse IgG (IgG) on chromatin from YAP-overexpressing hepatocytes. The STAT3 consensus region embedded in the *Snail* gene promoter and the TEAD consensus region embedded in the *Ctgf* gene promoter were analyzed. A TEAD unbounded region of the *RPL30* promoter was utilized as a negative control. Data are normalized to total chromatin input and background (control immunoprecipitation with IgG) and expressed as fold of enrichment. Mean ± SEM of qPCR data obtained from three independent experiment is reported.
D RT-qPCR analysis of the indicated YAP target genes in YAP-overexpressing and control HuH7 cells, treated with 5μM Stattic or 10μM of YAP-TEAD inhibitor Verteporfin (VP) or both, or with DMSO. The values are calculated by the 2(−ΔCt) method and shown as means ± S.E.M. of three independent experiments. Statistically significant differences are reported (*$p < 0.05$; **$p < 0.01$; ns= not significant).

Overall, the data shown so far demonstrate a functional cooperation between YAP and STAT3, where STAT3 positively affects both YAP expression and function. Moreover, the STAT3/YAP/TEAD co-occupancy on the CTGF promoter and the

equal contribution of STAT3 and TEAD to YAP-dependent gene expression suggest a possible epistatic functional relationship between these proteins.

3. ERK5 regulates the DNA binding of the YAP/STAT3 complex

Starting from our previous data, demonstrating in liver cells that ERK5 activity is required for the formation and the transcriptional activity of the YAP/TEAD complex (Ippolito F and Consalvi V, et al., 2023), we hypothesized the possible involvement of ERK5 also in controlling YAP/STAT3 complex assembly and recruitment on DNA.

To this aim, co-immunoprecipitation experiments and ChIP assays in YAP and STAT3 overexpressing cells, treated or not with the MEK5/ERK5 chemical inhibitor BIX02189, have been carried out. As shown in Figure 5A, we provided evidence that YAP/STAT3 complex formation does not require ERK5 kinase activity.

Instead, a ChIP assay performed with antibody anti-STAT3 in hepatocytes showed a drastic reduction of the STAT3 recruitment on both Snail (STAT3 consensus site) and CTGF (STAT3 and TEAD consensus sites) promoters in the presence of the ERK5 inhibitor

(Figure 5B), indicating a role for ERK5 in controlling DNA binding of the putative YAP/STAT3 complex (rather than in its formation). Interestingly, the DNA binding of TEAD to the same consensus site is not dependent on ERK5 activity (Figure 5C).

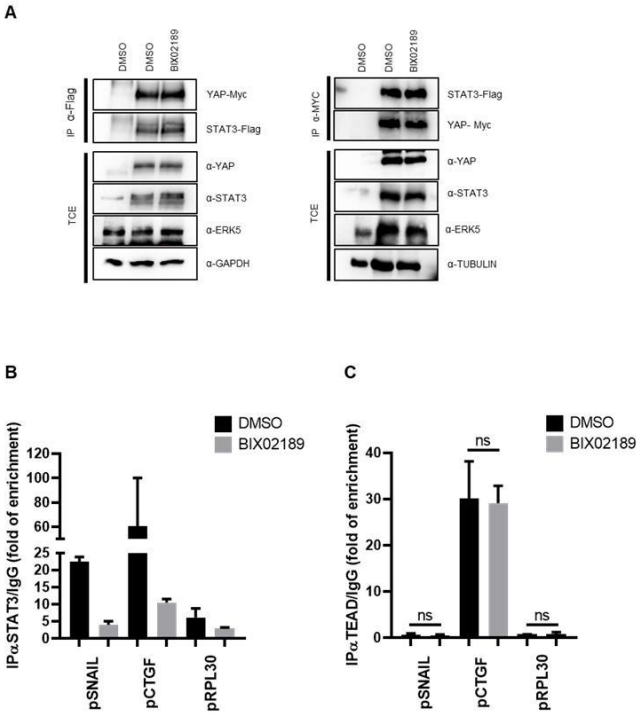

Figure 5

A. Co-immunoprecipitation of YAP and STAT3 proteins in HuH7 cells overexpressing $STAT3^{Flag}$ and $YAP^{Myc.}$, treated with 10 μM BIX02189 or with DMSO for 16 h. **Left** Total cell extracts (TCEs) and anti-Flag immunoprecipitates (IP) were analyzed by immunoblotting with anti-YAP and anti-STAT3 antibodies. GAPDH has been utilized as a loading control

of TCEs. WB images represent one indicative experiment of three independent ones. **Right** Total cell extracts (TCEs) and anti-Myc tag immunoprecipitates (IP) were analyzed by immunoblotting with anti-YAP and anti-STAT3 antibodies. Tubulin has been utilized as a loading control of TCEs. WB images represent one indicative experiment of three independent ones.

B. qPCR analysis of ChIP assays with anti-STAT3 antibody (IP) and, as control, normal mouse IgG (IgG) on chromatin from YAP-overexpressing hepatocytes treated with 20 μM BIX02189 or with DMSO for 16 h. The STAT3 consensus region embedded in the *Snail* gene promoter and the TEAD consensus region embedded in the *Ctgf* gene promoter were analyzed. A STAT3 unbounded region of the *RPL30* promoter was utilized as a negative control. Data are normalized to total chromatin input and background (control immunoprecipitation with IgG) and expressed as fold of enrichment. Mean ± SEM of qPCR data obtained in duplicate from two independent experiments is reported.

C. qPCR analysis of ChIP assays with anti-TEAD antibody (IP) and, as control, normal mouse IgG (IgG) on chromatin from YAP-overexpressing hepatocytes treated with 20 μM BIX02189 or with DMSO for 16 h. The STAT3 consensus region embedded in the *Snail* gene promoter and the TEAD consensus region embedded in the *Ctgf* gene promoter were analyzed. A TEAD unbounded region of the *RPL30* promoter was utilized as a negative control. Data are normalized to total chromatin input and background (control immunoprecipitation with IgG) and expressed as fold of enrichment. Mean ± SEM of qPCR data obtained from three independent experiments is reported. Statistically significant differences are reported (ns= not significant).

4. ERK5 drives a multilevel regulation of YAP interactome

In our previous published data obtained in hepatoma cells we gathered evidence that ERK5 modulates YAP-dependent gene expression and function (i.e. YAP-induced cell motility) at least in part, independently from Hippo/LATS pathway, since its inactivation could interfere with the activity of a mutated form of YAP protein, named YAP5SA, known to be resistant to the Hippo pathway-mediated inhibitory regulation (Figure 6 and data not shown). In particular, the substitution of five residues of serine with alanine in the protein impairs LATS1/2-induced inactivating phosphorylations (Zhao B et al. 2007).

Based on the results described above and our previous data demonstrating a role of ERK5 in the formation of YAP interactome and in the recruitment of YAP-including transcriptional complexes on DNA, we aimed at deeper investigating at molecular level the LATS-independence of these ERK5 functions.

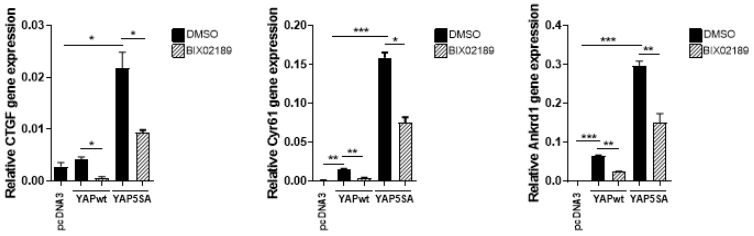

Figure 6
RT-qPCR analysis of the indicated YAP target genes in YAPwt or mutant YAP5SA-overexpressing HuH7 cells and control cells (pcDNA3), treated with 10 μM BIX02189 or DMSO. Data are expressed as relative gene expression and shown as mean ± S.E.M. of three independent experiments. Statistically significant differences are reported (*$p < 0.05$; **$p < 0.01$; ***$p < 0.001$).

Since in the co-IP described above we found that YAP/STAT3 complex is not dependent on ERK5 activity, while our previously published data showed that BIX02189 interferes with the YAP wild-type physical interaction with TEAD4 and its binding to CTGF promoter (Ippolito, Consalvi et al., 2023), we investigated the physical interaction between YAP5SA and TEAD4 and the binding to DNA in the presence of ERK5 chemical inhibition.

Figure 7A shows the results of Co-IPs performed in HuH7 cells treated with BIX02189 and overexpressing wild-type YAP or YAP5SA mutant protein. While the presence of the BIX02189 inhibitor impaired the interaction between YAPwt and TEAD4 as

previously described, it did not affect the interaction between YAP5SA and TEAD4.

Furthermore, a ChIP assay anti-YAP on chromatins from the HUH7 cell line overexpressing YAP5SA and treated with BIX02189 revealed that the binding of YAP5SA to the TEAD consensus region in the CTGF promoter was not affected (Figure 7B, left panel), differently from what was observed for the wild-type protein (Ippolito, Consalvi et al., 2023 and Figure 7B, right panel). Altogether, these results suggest that ERK5 drives a multilevel YAP-activity regulation that could involve Hippo-dependent and Hippo- independent mechanisms.

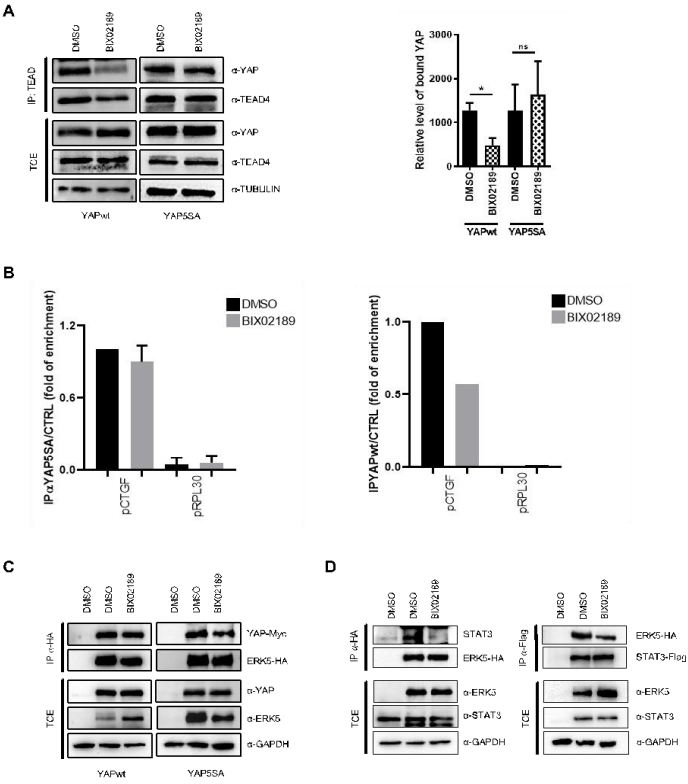

Figure 7

A Left Co-immunoprecipitation of YAP and TEAD proteins in HuH7 overexpressing, YAPwt, or YAP5SA was treated with BIX02189 or DMSO for 16h. Total cell extracts (TCEs) and anti-TEAD4 immunoprecipitates (IP) were analyzed by immunoblotting with anti-YAP and anti-TEAD4 antibodies. Tubulin has been utilized as a loading control of TCEs. WB images represent one indicative experiment of three independent ones. **Right** anti-YAP IP from three independent experiments was quantified by densitometric analysis and normalized on the relative anti-TEAD4 IP. Statistical significance: $*p < 0.05$; ns, not significant.

B qPCR analysis of ChIP assays with anti-Flag in HuH7 YAPwt^{Flag} or

YAP5SA^{Flag} overexpressing cells and, as control, pcDNA3 cells treated with BIX02189 or with DMSO for 16 h. The TEAD consensus region embedded in the *Ctgf* gene promoter was analyzed. A YAP unbounded region of the *RPL30* promoter was utilized as a negative control. Data are normalized to total chromatin input and background (control immunoprecipitation) and expressed as IP/CTRL. Right panel shows data from one single experiment in duplicate. In the left panel is reported mean ± SEM of qPCR data obtained in duplicate from two independent experiments.
C Co-immunoprecipitation of YAP and ERK5 proteins in HuH7 overexpressing YAPwt or YAP5SA and ERK5-HA, and treated with BIX02189 or DMSO for 16h. Total cell extracts (TCEs) and anti-HA immunoprecipitates (IP) were analyzed by immunoblotting with anti-YAP and anti-ERK5 antibodies. GAPDH has been utilized as a loading control of TCEs. WB images represent one indicative experiment of two independent ones.
D. Co-immunoprecipitation of ERK5 and STAT3 proteins in HuH7 cells overexpressing ERK5^{HA} and STAT3^{Flag}. **Left** Total cell extracts (TCEs) and anti-HA immunoprecipitates (IP) were analyzed by immunoblotting with anti-ERK5 and anti-STAT3 antibodies. GAPDH has been utilized as a loading control of TCEs. WB images represent one indicative experiment of two independent ones. **Right** Total cell extracts (TCEs) and anti-Flag immunoprecipitates (IP) were analyzed by immunoblotting with anti-ERK5 and anti-STAT3 antibodies. GAPDH has been utilized as a loading control of TCEs. WB images represent one indicative experiment of two independent ones.

Since ERK5 protein, unlike other MAPKs, possesses a transcriptional transactivation domain potentially able to interact with and bind transcription factors on the DNA (Kasler HG et al., 2000; Madak-Erdogan et al., 2014), it could be hypothesized its recruitment in the chromatin context. Currently, ChIP assays are underway to demonstrate this hypothesis. Meanwhile, co-IP

experiments in HuH7 cells overexpressing STAT3 together with YAP and ERK5 unveiled the physical interaction of ERK5 both with YAP (wild-type and mutant) and with STAT3 (Figure 7C and 7D) while no interaction with TEAD was observed (data not shown). Interestingly, we found that the treatment of cells with the ERK5 inhibitor interfered with STAT3/ERK5 interaction but not with YAP/ERK5 association (Figure 7C and 7D). These results support the hypothesis that ERK5 could be part of YAP-enrolled transcriptional complexes on the DNA and that its kinase activity is required for complex dynamics.

5. ERK5 activity modifies the YAP phosphorylation profile.

To investigate the mechanism by which ERK5 kinase activity controls YAP interactome and function, we firstly investigated whether the phosphorylation state of YAP was correlated with, or dependent on, the ERK5 kinase activity. The phosphorylation profile of YAP in HuH7 cells treated or not with BIX02189 inhibitor was analyzed by WB after electrophoresis in PhosTag gels conditioned with Mg2+ ions, able to separate phosphorylated proteins from their unphosphorylated counterparts. As shown in Figure 8A, HuH7 treated with the ERK5 inhibitor showed a significant decrease in YAP phosphorylation, while the phosphorylation profile of TEAD did not show any modification.

To confirm this result, we performed experiments in HuH7 cells treated with nocodazole, a mitosis inhibitor known to induce ERK5 activation (Cude K et al., 2007). Figure 8B shows that the increase of ERK5 activity (assessed on an ERK5-dependent MEF2-responsive promoter driving a luciferase gene) (Woronicz JD et al., 1995), after nocodazole treatment correlates with the activation of YAP (assessed on a YAP-dependent TEAD-responsive promoter in luc-assay) (Dupont S et al., 2011) and the transcription of endogenous target genes. Notably, we found a strong ERK5-

dependent YAP-phosphorylation induced by the nocodazole, since it is almost completely lost after treatment with BIX02189. Of note, in this experimental condition, TEAD and STAT3 did not result phosphorylated (Figure 8C), suggesting that YAP, but not TEAD or STAT3, is the putative target of ERK5 kinase activity.

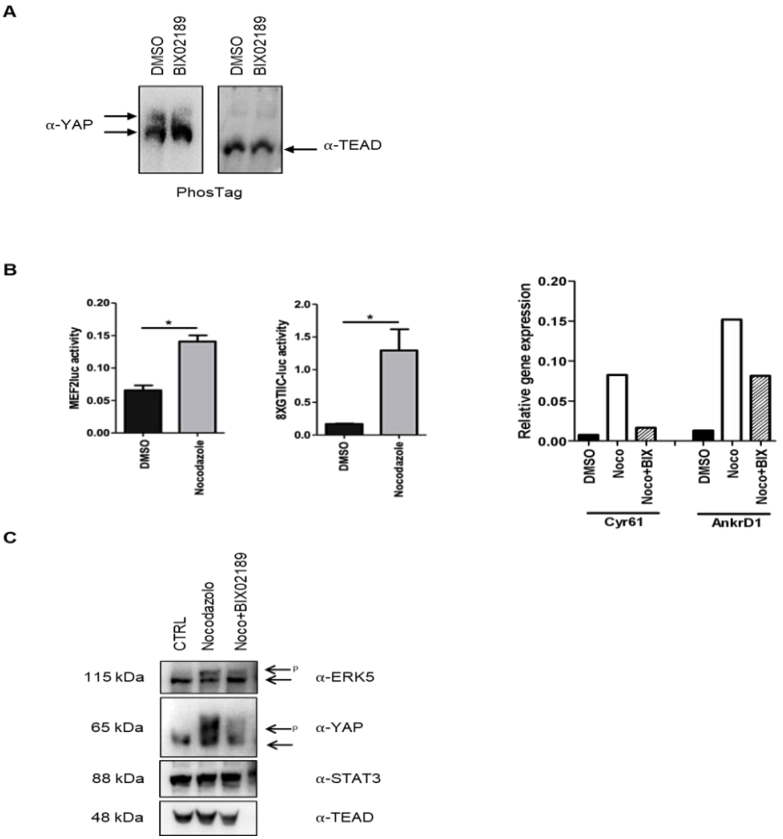

Figure 8
A. PhosTag western blot for the indicated proteins in HuH7 treated with 10 μM BIX02189 for 16h. Phostag gel conditioned with Mg2+ ions can slow down phosphorylated proteins during the run and separate them from the total amount of protein. WB images represent one indicative experiment of two independent ones.
B. Luciferase assay. **Left** MEF2-luc or 8xGTIIC-luc reporters were transiently co-transfected in HuH7 cells with a Renilla expression vector. Cells were treated with nocodazole for 24h. Luciferase activities were normalized for Renilla luciferase activity and expressed as arbitrary units. Statistically significant differences are reported. **Right** RT-qPCR analysis of the indicated YAP target genes in HuH7 treated with nocodazole or with nocodazole and BIX02189. The values are calculated by the 2(−ΔCt) method and shown as means ± S.E.M. A single experiment is shown.
C. PhosTag western blot for the indicated proteins in HuH7 treated with nocodazole or with nocodazole and BIX02189. WB images represent one indicative experiment of two independent ones.

Thus, to clarify whether YAP protein could be a direct target of ERK5 kinase, we executed an in *vitro* kinase assay utilizing an active recombinant form of ERK5 together with YAP, TEAD, and STAT3 *in vitro* translated (IVT) proteins (with or without calf intestinal phosphatase, CIP). Figure 9A shows a Phos-tag WB analysis where a slight phosphorylation of YAP appears in the sample with active ERK5 (not present in the CIP-treated sample). In contrast, no modification of the phosphorylation state of STAT3 and TEAD can be observed. To exclude a non-specific phosphorylation due to the high amount of the kinase in the *in vitro* assay and in the hypothesis that the YAP phosphorylation

by ERK5 could require priming post-translational modifications (PTM) by other enzymes or the presence of cofactors, the kinase assay has been carried out on YAP protein immunoprecipitated from YAP overexpressing HuH7 cells, treated or not with BIX02189 inhibitor. In WB the phosphorylation state of YAP has been analyzed by the use of an anti-serine antibody. As shown in Figure 9B (left panels), recombinant ERK5 induced a strong increase in serine phosphorylation of YAP (Figure 9B). As a control, the autophosphorylation of the active kinase is also shown. Of note, ERK5 can phosphorylate also the immunoprecipitated YAP protein from BIX02189-treated cells, suggesting that the eventual cofactor or priming PTM that allows a sustained YAP phosphorylation by ERK5 is not dependent on the kinase. In the attempt to identify YAP interactors that could account for this result and putative ERK5-targeted serine residues on YAP protein, a proteomic analysis on immunoprecipitated YAP protein in condition of ERK5 inactivation (by chemical inhibition) or sustained activation (by overexpression) is ongoing. This analysis will clarify the biochemical requirements for ERK5-induced phosphorylation.

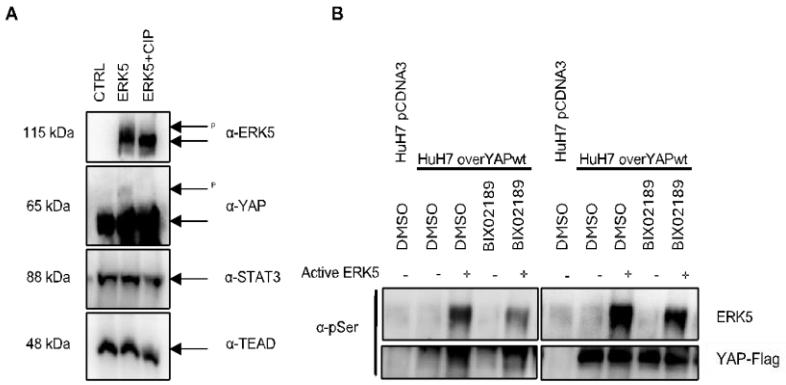

Figure 9
A Western blot with PhosTag gels for the indicated proteins. Samples used were derived from an *in vitro* translated protein (IVT) kinase assay. IVT YAP was incubated with active ERK5 or ERK5 and CIP. WB images represent one indicative experiment.
B HuH7 cells over-expressing wtYAP^{Flag} and control cells (pcDNA3) were treated with BIX02189 or DMSO for 16h. The cell lysates were immunoprecipitated with anti-Flag antibody, and then a kinase assay with active ERK5 was performed on the immunoprecipitate. Then, the samples were run on WB and hybridized with anti-pSer, anti-YAP, or anti-ERK5 antibodies. WB images represent one indicative experiment.

According to the *in vitro* kinase assay, the analysis of putative kinases targeting YAP protein by the PhosphositePlus Kinase Prediction database indicated several amino acid residues (Thr77, Ser217, Ser227, Ser289, and Ser367) as possible ERK5 phosphorylation target sites with high predictive scores,

supporting the hypothesis that YAP is a direct target of ERK5 kinase activity. Notably, some of these predicted serine residues (i.e. Ser289 and Ser 367) on YAP protein were found to be associated in a quantitative phosphoproteomic analysis with nocodazole treatment (Olsen JV et al., 2010). This evidence supports the findings of YAP as a new substrate of ERK5 kinase, even if further analysis will be required for the formal demonstration of this.

6. lncRNA MALAT1 binds to YAP in an ERK5-dependent manner and is required for YAP target gene expression.

Recent literature indicates that lncRNAs may play a crucial role in the structure and function of molecular platforms driven by master transcription factors on DNA as scaffolds for specific epigenetic regulators (Battistelli et al., 2017). Therefore, a bioinformatics analysis by the RPISeq online tool (http://pridb.gdcb.iastate.edu/RPISeq/index.html) was performed to identify putative YAP-interacting lncRNAs with a possible role as components of its transcriptional platforms. High predictor scores were obtained for the interaction between YAP and two lncRNAs, i.e., MALAT1 and NEAT1.

RNA immunoprecipitation (RIP) analyses were performed in HuH7 cells overexpressing YAP wild-type protein to validate these data. As shown in Figure 10A, YAP was found to interact with MALAT1 but not with NEAT1 (data not shown) in this cell line. Instead, no interaction was observed between MALAT1 and TEAD (data not shown).

In the hypothesis of a role for MALAT1 in the regulation of the YAP activity, we first analyzed the expression of this lncRNA in liver cell

models where YAP functional role has been well characterized and correlated with the differentiation status.

In the undifferentiated liver precursor cell line RLSCs, exhibiting high levels of YAP mainly localized in the nucleus and in an active form (Cozzolino et al., 2016), high levels of MALAT1 were observed (Figure 10B). In contrast, in the terminally differentiated hepatocyte cell line HepD3, low levels of YAP protein, predominantly cytoplasmic and inactive, correlate to low levels of MALAT1 (Figure 10B).

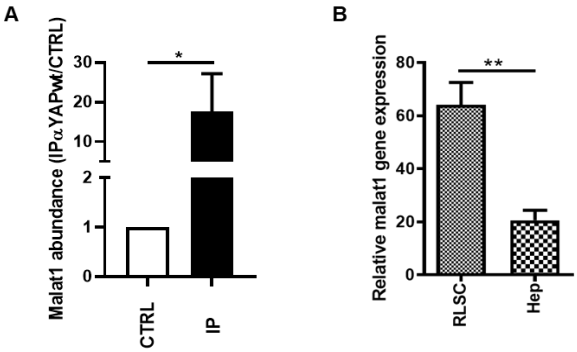

Figure 10

A. RT-qPCR analysis of RIP assays with anti-YAP (IP) in YAP-overexpressing HuH7 cells and, as control, with anti-rabbit IgG. The MALAT1 RNA was analyzed. A YAP unbounded RNA, *RPL34,* was utilized as a negative control. Data are normalized to total chromatin input and background RPL34. Mean ± SEM of qPCR data obtained from three

independent experiments is reported. Statistical significance: *$p < 0.05$.
B. RT-qPCR analysis of MALAT1 gene expression in liver progenitor RLSC cells or in hepatocytes. Data are expressed as relative gene expression and shown as mean ± S.E.M. of three independent experiments. Statistically significant differences are reported (**$p < 0.01$).

Then, to evaluate whether the expression levels of MALAT1 and YAP were only correlative or whether the lncRNA was needed for the regulation of YAP activity, experiments of MALAT1 silencing were performed in YAP-overexpressing HuH7 cells. To interfere with MALAT1 expression, two different siRNAs have been utilized. As shown in Figure 11A, both siRNAs significantly reduced its expression. The YAP target genes CTGF and Cyr61 expression were significantly downregulated in these conditions. Of note, YAP overexpression did not impact MALAT1 expression. Since the YAP protein level, assessed by WB (Figure 11B), was not affected by the silencing of MALAT1, we speculated that the lncRNA could be required for its transcriptional activity on specific target genes (indeed, the expression of Ankrd1, another well-known YAP target gene, has not been downregulated).

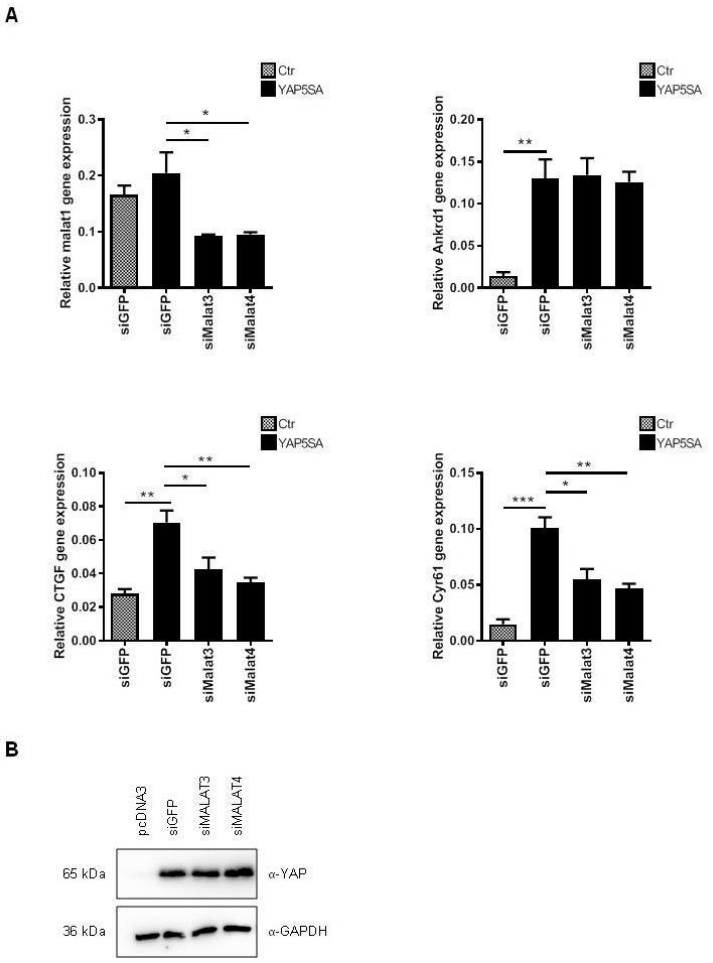

Figure 11

A. RT-qPCR analysis of the indicated YAP target genes in YAP-overexpressing HuH7 cells (YAP5SA) and control cells (pcDNA3) silenced with siMALAT3, siMALAT4, or control siGFP. Data are expressed as

relative gene expression and shown as mean ± S.E.M. of three independent experiments. Statistically significant differences are reported (*$p < 0.05$; **$p < 0.01$; ***$p < 0.001$).
B. Western blot for YAP in YAP-overexpressing HuH7 cells (YAP5SA) and control cells (pcDNA3) silenced with siMALAT3, siMALAT4, or control siGFP. GAPDH has been utilized as a loading control.

In the hypothesis of a role for ERK5 in the MALAT1/YAP interaction, we performed an RNA immunoprecipitation (RIP) analysis in HuH7 cells overexpressing YAP wild-type protein and silenced or not with shERK5. As shown in Figure 12, YAP was found to interact with MALAT1 and the interaction was lost silencing ERK5.

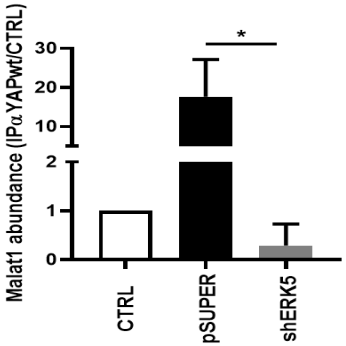

Figure 12
RT-qPCR analysis of RIP assays with anti-Flag (YAP^{Flag}) in pcDNA3 transfected HuH7 cells (CTRL) or in $wtYAP^{Flag}$-overexpressing HuH7 cells transfected with pSUPER-shERK5 or the empty vector. The MALAT1 RNA was analyzed 48 h post-transfection. A YAP unbounded RNA, *RPL34*, was

utilized as a negative control. Data are normalized to total chromatin input and background RPL34. Mean ± SEM of qPCR data obtained from three independent experiment is reported. Statistical significance: *p < 0.05.

Overall, we described a role for the lncRNA MALAT1 in YAP-dependent target gene expression in hepatoma cells. Moreover, the findings of the ERK5-dependent MALAT1/YAP interaction and the regulation MALAT1-dependent of CTGF and Cyr61 genes (where we previously showed the binding of the putative YAP/STAT3/TEAD complex,) support the hypothesis that YAP could recruit the lncRNA on target gene promoters.

CONCLUSIONS AND PERSPECTIVES

Despite several reports highlighting the pivotal role of YAP in cancer, how it can mediate tissue- and cell context-dependent gene expression and determine different tumorigenic processes remains to be clarified.

Growing evidence suggests that the pleiotropic function of YAP can be ascribed to the composition and genome occupancy of transcriptional complexes that it can enroll, in driving specific gene expression and functional outcome. This implies that the identification of YAP partners in chromatin context and the clarification of their regulation could be considered in cancer therapy, often just limited by the tumor histotype-specificity (Lopez-Hernandez A. et al., 2021).

We previously demonstrated, in liver cells, the physical interaction between YAP and the transcriptional factor STAT3 and their co-occupancy of a promoter region of Snail, the master gene of the epithelial-to-mesenchymal transition (EMT) and driver of tumor progression in several human cancers (Noce et al., 2019).

These findings, coupled to the well-known oncogenic role of

STAT3 in controlling gene expression in proliferation, survival, migration and, notably, tumor progression (Sadrkhanloo M et al., 2022; Guanizo AC et al., 2018) prompted us to investigate the possible role of STAT3 in mediating YAP-dependent transcriptional activation in hepatoma cells.

The here provided results demonstrated the physical interaction between STAT3 and YAP, as well as the requirement of STAT3 for the functional activity of YAP. Additionally, it was observed that STAT3 is required for the transcription of YAP target genes, CTGF and CYR61, previously reported in the literature as targets of YAP/TEAD complex.

Our data showed a transcriptional cooperation between STAT3 and TEAD in the regulation of YAP target genes, as suggested also by bioinformatic data showing an overlap between peaks of chromatin occupancy, that we found to be epistatic.

In a recent study, we unveiled ERK5/MAPK as a new regulator of YAP transcriptional activity. In particular, we demonstrated that ERK5 activity is required for the maintenance of YAP transcriptional activity and the upregulation of specific target genes in human hepatocellular carcinoma cell lines.

Mechanistically, data obtained in this work showed that ERK5

regulates YAP/STAT3 DNA binding and function while it is dispensable for their physical interaction. Moreover, our data indicates that ERK5 can interact both with STAT3 and YAP but its kinase activity is required only for the interaction with STAT3. This finding suggests a role for ERK5 as a structural, other than functional, element of YAP-enrolled transcriptional complex, shedding light on a still poorly explored nuclear function of this kinase.

As shown in our previous work, ERK5-induced regulation of YAP can interfere with the activity of a constitutively active YAP mutant, resistant to the LATS-induced inactivating phosphorylations, suggesting the independence of its signaling from Hippo pathway. We gathered evidence that, in the presence of ERK5 inhibition and differently from the wild- type YAP protein, the YAP5SA mutant maintains the ability to bind TEAD4 (Figure 7A) and DNA (Figure 7B) despite the detachment of STAT3 from the transcriptional complex (Figure 5B) and its functional inactivation (Figure 2).

Notably, we gathered evidence of a role of ERK5 as a direct kinase of YAP even if our data suggest that YAP phosphorylation by ERK5 could require additional regulations

(priming modifications and/or cofactors).

Altogether, these findings suggest the model depicted in Figure 12 where the formation of a multimeric complex enrolled by YAP is regulated by ERK5-induced phosphorylation and, possibly, by its transactivating activity.

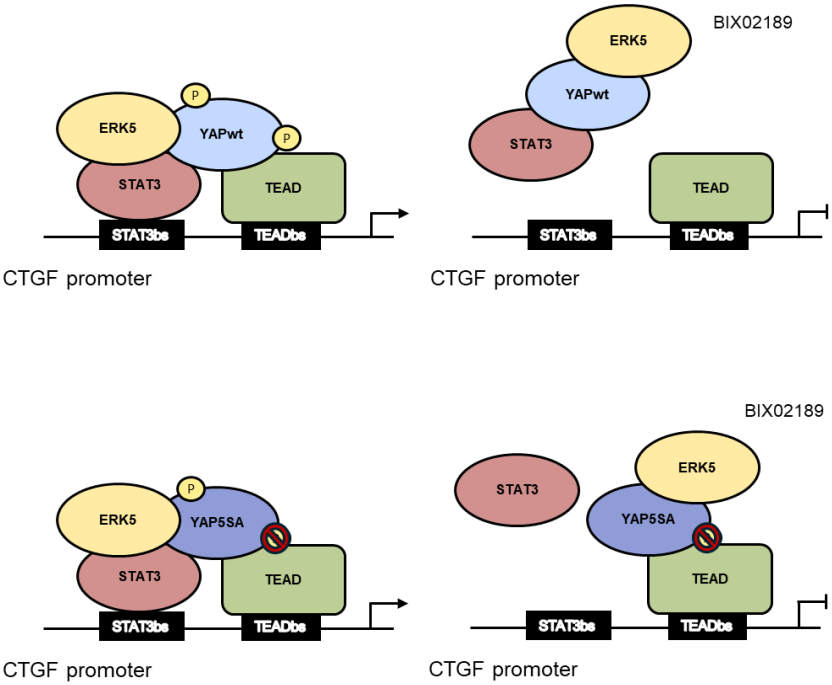

Figure 13. Model of the transcriptional regulation of CTGF gene by the YAP/TEAD/STAT3 transcriptional complexes

Upper panels. In the condition of ERK5 activation, the trimeric

YAP/TEAD/STAT3 complex is bound on STAT3 and TEAD binding sites embedded in the CTGF promoter, driving its transcriptional activation. The ERK5 kinase activity on YAP protein is required for the YAP/TEAD but not for YAP/STAT3 interaction. In this soluble complex, YAP/ERK5 interaction is maintained while a possible conformational change in YAP (or in other partners) drives the distancing between ERK5 and STAT3.
Lower panels Differently from the wild-type protein, YAP5SA mutant is constitutively bound to TEAD on its binding sites in the CTGF promoter. The inactivation of ERK5 by BIX02189 interferes with the binding of STAT3 to DNA.

The mechanisms proposed for the dynamic formation and activation of different transcriptional complexes, could be extended to other YAP target genes where interactions between proximal and distal transcription factors (i.e. STAT3 and TEAD) by means of chromatin loops can be hypothesized and the assembly of the protein components could include lncRNAs as scaffolds.

Based on our results, showing that lncMALAT1 can interact with YAP protein and is involved in the regulation of YAP-induced gene expression of target genes such as CTGF and Cyr61, we hypothesize that the lncRNA could be recruited by YAP in transcriptional complexes to bridge epigenetic regulators. Further study will shed light on this possible mechanism of action.

Overall, this study can provide new knowledge of how specific DNA binding partners of YAP and kinases regulating the complex formation and activity can dictate the selection of its target genes in cancer, and provide new translational insights into the mechanisms that regulate its activity in cancer, suggesting new possible molecular targets for its treatment.

BIBLIOGRAPHY

Abe, J., et al. (1996). "Big mitogen-activated protein kinase 1 (BMK1) is a redox-sensitive kinase." J Biol Chem 271(28): 16586-16590.

Adler, J. J., et al. (2013). "Serum deprivation inhibits the transcriptional co-activator YAP and cell growth via phosphorylation of the 130-kDa isoform of Angiomotin by the LATS1/2 protein kinases." Proc Natl Acad Sci U S A 110(43): 17368-17373.

Alder, O., et al. (2014). "Hippo signaling influences HNF4A and FOXA2 enhancer switching during hepatocyte differentiation." Cell Rep 9(1): 261-271.

Arnoux, V., et al. (2008). "Erk5 controls Slug expression and keratinocyte activation during wound healing." Mol Biol Cell 19(11): 4738-4749.

Bai, H., et al. (2016). "Yes-associated protein impacts adherens junction assembly through regulating actin cytoskeleton organization." Am J Physiol Gastrointest Liver Physiol 311(3): G396-411.

Barry, E. R., et al. (2013). "Restriction of intestinal stem cell expansion and the regenerative response by YAP." Nature 493(7430): 106-110.

Battistelli, C., et al. (2017). "The Snail repressor recruits EZH2 to specific genomic sites through the enrollment of the lncRNA HOTAIR in epithelial-to-mesenchymal transition." Oncogene 36(7): 942-955.

Bliss, S. P., et al. (2012). "ERK signaling, but not c-Raf, is required for gonadotropin-releasing hormone (GnRH)-induced regulation of Nur77 in pituitary gonadotropes." Endocrinology 153(2): 700-711.

Borten, M. A., et al. (2018). "Automated brightfield morphometry of 3D organoid populations by OrganoSeg." Sci Rep 8(1): 5319.

Brown, J. A., et al. (2014). "Structural insights into the stabilization of MALAT1 noncoding RNA by a bipartite triple helix." Nat Struct Mol Biol 21(7): 633-640.

Cai, J., et al. (2010). "The Hippo signaling pathway restricts the oncogenic potential of an intestinal regeneration program." Genes Dev 24(21): 2383-2388.

Calvo, F., et al. (2013). "Mechanotransduction and YAP-dependent matrix remodelling is required for the generation and maintenance of cancer-associated fibroblasts." Nat Cell Biol 15(6): 637-646.

Cao, J. and W. Huang (2017). "Two faces of Hippo: activate or suppress the Hippo pathway in cancer." Anticancer Drugs 28(10): 1079-1085.

Cao, S., et al. (2016). "Tumor-suppressive function of long noncoding RNA MALAT1 in glioma cells by suppressing miR-155 expression and activating FBXW7 function." Am J Cancer Res 6(11): 2561-2574.

Chan, S. W., et al. (2008). "A role for TAZ in migration, invasion, and tumorigenesis of breast cancer cells." Cancer Res 68(8): 2592-2598.

Chen, L. L. (2016). "Linking Long Noncoding RNA Localization and

Function." Trends Biochem Sci 41(9): 761-772.

Conigliaro, A., et al. (2013). "Evidence for a common progenitor of epithelial and mesenchymal components of the liver." Cell Death Differ 20(8): 1116-1123.

Conigliaro, A., et al. (2008). "Isolation and characterization of a murine resident liver stem cell." Cell Death Differ 15(1): 123-133.

Cordenonsi, M., et al. (2011). "The Hippo transducer TAZ confers cancer stem cell-related traits on breast cancer cells." Cell 147(4): 759-772.

Cozzolino, A. M., et al. (2013). "TGFbeta overrides HNF4alpha tumor suppressing activity through GSK3beta inactivation: implication for hepatocellular carcinoma gene therapy." J Hepatol 58(1): 65-72.

Cozzolino, A. M., et al. (2016). "Modulating the Substrate Stiffness to Manipulate Differentiation of Resident Liver Stem Cells and to Improve the Differentiation State of Hepatocytes." Stem Cells Int 2016: 5481493.

Croci, O., et al. (2017). "Transcriptional integration of mitogenic and mechanical signals by Myc and YAP." Genes Dev 31(20): 2017-2022.

Cude, K., et al. (2007). "Regulation of the G2-M cell cycle progression by the ERK5-NFkappaB signaling pathway." J Cell Biol 177(2): 253-264.

Dai, X., et al. (2013). "Phosphorylation of angiomotin by Lats1/2 kinases inhibits F-actin binding, cell migration, and angiogenesis." J Biol Chem 288(47): 34041-34051.

Di Agostino, S., et al. (2016). "YAP enhances the pro-proliferative transcriptional activity of mutant p53 proteins." EMBO Rep 17(2): 188-201.

Dinev, D., et al. (2001). "Extracellular signal regulated kinase 5 (ERK5) is required for the differentiation of muscle cells." EMBO Rep 2(9): 829-834.

Drew, B. A., et al. (2012). "MEK5/ERK5 pathway: the first fifteen years." Biochim Biophys Acta 1825(1): 37-48.

Dupont, S., et al. (2011). "Role of YAP/TAZ in mechanotransduction." Nature 474(7350): 179-183.

Eissmann, M., et al. (2012). "Loss of the abundant nuclear non-coding RNA MALAT1 is compatible with life and
Elbediwy, A., et al. (2016). "YAP and TAZ in epithelial stem cells: A sensor for cell polarity, mechanical forces and tissue damage." Bioessays 38(7): 644-653.

Erazo, T., et al. (2013). "Canonical and kinase activity-independent mechanisms for extracellular signal-regulated kinase 5 (ERK5) nuclear translocation require dissociation of Hsp90 from the ERK5-Cdc37 complex." Mol Cell Biol 33(8): 1671-1686.

Esparis-Ogando, A., et al. (2002). "Erk5 participates in neuregulin signal transduction and is constitutively active in breast cancer cells overexpressing ErbB2." Mol Cell Biol 22(1): 270-285.

Esteller, M. (2011). "Non-coding RNAs in human disease." Nat Rev Genet 12(12): 861-874.

Fan, Y., et al. (2014). "TGF-beta-induced upregulation of malat1

promotes bladder cancer metastasis by associating with suz12." Clin Cancer Res 20(6): 1531-1541.

Feng, X., et al. (2014). "Hippo-independent activation of YAP by the GNAQ uveal melanoma oncogene through a trio-regulated rho GTPase signaling circuitry." Cancer Cell 25(6): 831-845.

Fitamant, J., et al. (2015). "YAP Inhibition Restores Hepatocyte Differentiation in Advanced HCC, Leading to Tumor Regression." Cell Rep 10(10): 1692-1707.

Fouad, Y. A. and C. Aanei (2017). "Revisiting the hallmarks of cancer." Am J Cancer Res 7(5): 1016-1036.

Gan, X. Q., et al. (2008). "Nuclear Dvl, c-Jun, beta-catenin, and TCF form a complex leading to stabilization of beta-catenin-TCF interaction." J Cell Biol 180(6): 1087-1100.

Gao, C. and J. Peng (2021). "All routes lead to Rome: multifaceted origin of hepatocytes during liver regeneration." Cell Regen 10(1): 2.

Goldstein, I., et al. (2017). "Synergistic gene expression during the acute phase response is characterized by transcription factor assisted loading." Nat Commun 8(1): 1849.

Gregorieff, A., et al. (2015). "Yap-dependent reprogramming of Lgr5(+) stem cells drives intestinal regeneration and cancer." Nature 526(7575): 715-718.

Guanizo AC, et al. (2018) “STAT3: a multifaceted oncoprotein.” Growth Factors. 36(1-2):1-14.

Guo, F., et al. (2015). "Expression of MALAT1 in the peripheral

whole blood of patients with lung cancer." Biomed Rep 3(3): 309-312.

Hao, Y., et al. (2020). "IL-6/STAT3 mediates the HPV18 E6/E7 stimulated upregulation of MALAT1 gene in cervical cancer HeLa cells." Virus Res 281: 197907.

Harvey, K. F., et al. (2013). "The Hippo pathway and human cancer." Nat Rev Cancer 13(4): 246-257.

Heallen, T., et al. (2011). "Hippo pathway inhibits Wnt signaling to restrain cardiomyocyte proliferation and heart size." Science 332(6028): 458-461.

Huang, Z., et al. (2016). "YAP stabilizes SMAD1 and promotes BMP2-induced neocortical astrocytic differentiation." Development 143(13): 2398-2409.

Ippolito, F., et al. (2023). "Extracellular signal-Regulated Kinase 5 (ERK5) is required for the Yes-associated protein (YAP) co-transcriptional activity." Cell Death Dis 14(1): 32.

Itoh, K., et al. (2005). "Nuclear localization is required for Dishevelled function in Wnt/beta-catenin signaling." J Biol 4(1): 3.

Kamakura, S., et al. (1999). "Activation of the protein kinase ERK5/BMK1 by receptor tyrosine kinases. Identification and characterization of a signaling pathway to the nucleus." J Biol Chem 274(37): 26563-26571.

Kapranov, P., et al. (2007). "RNA maps reveal new RNA classes and a possible function for pervasive transcription." Science 316(5830):

1484-1488.

Kasler, H. G., et al. (2000). "ERK5 is a novel type of mitogen-activated protein kinase containing a transcriptional activation domain." Mol Cell Biol 20(22): 8382-8389.

Kato, Y., et al. (1997). "BMK1/ERK5 regulates serum-induced early gene expression through transcription factor MEF2C." EMBO J 16(23): 7054-7066.

Kim, J., et al. (2018). "Long noncoding RNA MALAT1 suppresses breast cancer metastasis." Nat Genet 50(12): 1705-1715.

Kim, M., et al. (2015). "Transcriptional co-repressor function of the hippo pathway transducers YAP and TAZ." Cell Rep 11(2): 270-282.

Kim, N. G., et al. (2011). "E-cadherin mediates contact inhibition of proliferation through Hippo signaling-pathway components." Proc Natl Acad Sci U S A 108(29): 11930-11935.

Kotake, Y., et al. (2011). "Long non-coding RNA ANRIL is required for the PRC2 recruitment to and silencing of p15(INK4B) tumor suppressor gene." Oncogene 30(16): 1956-1962.

Kwok, Z. H., et al. (2018). "A non-canonical tumor suppressive role for the long non-coding RNA MALAT1 in colon and breast cancers." Int J Cancer 143(3): 668-678.

Latorre, E., et al. (2016). "The Ribonucleic Complex HuR-MALAT1 Represses CD133 Expression and Suppresses Epithelial-Mesenchymal Transition in Breast Cancer." Cancer Res 76(9): 2626-2636.

Lehmann, W., et al. (2016). "ZEB1 turns into a transcriptional activator by interacting with YAP1 in aggressive cancer types." Nat Commun 7: 10498.

Levy, D., et al. (2007). "The Yes-associated protein 1 stabilizes p73 by preventing Itch-mediated ubiquitination of p73." Cell Death Differ 14(4): 743-751.

Li, H., et al. (2012). "Deregulation of Hippo kinase signalling in human hepatic malignancies." Liver Int 32(1): 38-47.

Li, M. M., et al. (2019). "LncRNA-MALAT1 promotes tumorogenesis of infantile hemangioma by competitively binding miR-424 to stimulate MEKK3/NF-kappaB pathway." Life Sci 239: 116946.

Li, Q., et al. (2016). "Disrupting MALAT1/miR-200c sponge decreases invasion and migration in endometrioid endometrial carcinoma." Cancer Lett 383(1): 28-40.

Li Y, Wang Z, Shi H, Li H, Li L, Fang R, et al. HBXIP and LSD1 Scaffolded by lncRNA Hotair Mediate Transcriptional Activation by c-Myc. Cancer Res. 2016;76(2):293-304.

Li, Z., et al. (2012). "6 Paths of ERK5 signaling pathway regulate hepatocyte proliferation in rat liver regeneration." Indian J Biochem Biophys 49(3): 165-172.

Li, Z. X., et al. (2018). "MALAT1: a potential biomarker in cancer." Cancer Manag Res 10: 6757-6768.

Liu, C. Y., et al. (2016). "MRTF/SRF dependent transcriptional regulation of TAZ in breast cancer cells." Oncotarget 7(12): 13706-13716.

Liu, S., et al. (2018). "Knockdown of Long Noncoding RNA (lncRNA) Metastasis-Associated Lung Adenocarcinoma Transcript 1 (MALAT1) Inhibits Proliferation, Migration, and Invasion and Promotes Apoptosis by Targeting miR-124 in Retinoblastoma." Oncol Res 26(4): 581-591.

Liu, X., et al. (2013). "PTPN14 interacts with and negatively regulates the oncogenic function of YAP." Oncogene 32(10): 1266-1273.

Liu, Y., et al. (2017). "YAP modulates TGF-beta1-induced simultaneous apoptosis and EMT through upregulation of the EGF receptor." Sci Rep 7: 45523.

Liu-Chittenden, Y., et al. (2012). "Genetic and pharmacological disruption of the TEAD-YAP complex suppresses the oncogenic activity of YAP." Genes Dev 26(12): 1300-1305.

Lopez-Hernandez, A., et al. (2021). "Emerging Principles in the Transcriptional Control by YAP and TAZ." Cancers (Basel) 13(16).

Low, B. C., et al. (2014). "YAP/TAZ as mechanosensors and mechanotransducers in regulating organ size and tumor growth." FEBS Lett 588(16): 2663-2670.

Madak-Erdogan, Z., et al. (2014). "Novel roles for ERK5 and cofilin as critical mediators linking ERalpha-driven transcription, actin reorganization, and invasiveness in breast cancer." Mol Cancer Res 12(5): 714-727.

Mana-Capelli, S., et al. (2014). "Angiomotins link F-actin architecture to Hippo pathway signaling." Mol Biol Cell 25(10): 1676-1685.

Marchetti, A., et al. (2008). "ERK5/MAPK is activated by TGFbeta in hepatocytes and required for the GSK-3beta-mediated Snail protein stabilization." Cell Signal 20(11): 2113-2118.

McDaniel, J. M., et al. (2017). "Genomic regulation of invasion by STAT3 in triple negative breast cancer." Oncotarget 8(5): 8226-8238.
Mehta, P. B., et al. (2003). "MEK5 overexpression is associated with metastatic prostate cancer, and stimulates proliferation, MMP-9 expression and invasion." Oncogene 22(9): 1381-1389.

Meng, Z., et al. (2016). "Mechanisms of Hippo pathway regulation." Genes Dev 30(1): 1-17.

Meng, Z., et al. (2015). "MAP4K family kinases act in parallel to MST1/2 to activate LATS1/2 in the Hippo pathway." Nat Commun 6: 8357.

Mercer TR, Dinger ME, Mattick JS. Long non-coding RNAs: insights into functions. Nat Rev Genet. 2009;10(3):155-9.

Mercer, T. R. and J. S. Mattick (2013). "Structure and function of long noncoding RNAs in epigenetic regulation." Nat Struct Mol Biol 20(3): 300-307.

Metcalfe, C., et al. (2010). "Dvl2 promotes intestinal length and neoplasia in the ApcMin mouse model for colorectal cancer." Cancer Res 70(16): 6629-6638.

Mo, J. S., et al. (2014). "The Hippo signaling pathway in stem cell biology and cancer." EMBO Rep 15(6): 642-656.

Morimoto, H., et al. (2007). "Activation of a C-terminal transcriptional activation domain of ERK5 by

autophosphorylation." J Biol Chem 282(49): 35449-35456.

Moroishi, T., et al. (2015). "The emerging roles of YAP and TAZ in cancer." Nat Rev Cancer 15(2): 73-79.

Noce, V., et al. (2019). "YAP integrates the regulatory Snail/HNF4alpha circuitry controlling epithelial/hepatocyte differentiation." Cell Death Dis 10(10): 768.

Oh, H., et al. (2013). "Genome-wide association of Yorkie with chromatin and chromatin-remodeling complexes." Cell Rep 3(2): 309-318.

Oh, H., et al. (2014). "Yorkie promotes transcription by recruiting a histone methyltransferase complex." Cell Rep 8(2): 449-459.

Olsen, J. V., et al. (2010). "Quantitative phosphoproteomics reveals widespread full phosphorylation site occupancy during mitosis." Sci Signal 3(104): ra3.

Ortega, A., et al. (2021). "The YAP/TAZ Signaling Pathway in the Tumor Microenvironment and Carcinogenesis: Current Knowledge and Therapeutic Promises." Int J Mol Sci 23(1).

Pan, D. (2010). "The hippo signaling pathway in development and cancer." Dev Cell 19(4): 491-505.

Pan, J. X., et al. (2018). "YAP promotes osteogenesis and suppresses adipogenic differentiation by regulating beta-catenin signaling." Bone Res 6: 18.

Peng, N., et al. (2020). "Long noncoding RNA MALAT1 inhibits the apoptosis and autophagy of hepatocellular carcinoma cell by

targeting the microRNA-146a/PI3K/Akt/mTOR axis." Cancer Cell Int 20: 165.

Pi, X., et al. (2004). "Big mitogen-activated protein kinase (BMK1)/ERK5 protects endothelial cells from apoptosis." Circ Res 94(3): 362-369.

Pinto, D., et al. (2003). "Canonical Wnt signals are essential for homeostasis of the intestinal epithelium." Genes Dev 17(14): 1709-1713.

Prensner, J. R. and A. M. Chinnaiyan (2011). "The emergence of lncRNAs in cancer biology." Cancer Discov 1(5): 391-407.

Qing, Y., et al. (2014). "The Hippo effector Yorkie activates transcription by interacting with a histone methyltransferase complex through Ncoa6." Elife 3.

Ramsay, A. K., et al. (2011). "ERK5 signalling in prostate cancer promotes an invasive phenotype." Br J Cancer 104(4): 664-672.

Regan, C. P., et al. (2002). "Erk5 null mice display multiple extraembryonic vascular and embryonic cardiovascular defects." Proc Natl Acad Sci U S A 99(14): 9248-9253.

Roberts, O. L., et al. (2010). "ERK5 is required for VEGF-mediated survival and tubular morphogenesis of primary human microvascular endothelial cells." J Cell Sci 123(Pt 18): 3189-3200.

Rovida, E., et al. (2015). "The mitogen-activated protein kinase ERK5 regulates the development and growth of hepatocellular carcinoma." Gut 64(9): 1454-1465.

Rovida, E., et al. (2008). "ERK5/BMK1 is indispensable for optimal colony-stimulating factor 1 (CSF-1)-induced proliferation in macrophages in a Src-dependent fashion." J Immunol 180(6): 4166-4172.

Sadrkhanloo M, et al. (2022) “STAT3-EMT axis in tumors: Modulation of cancer metastasis, stemness and therapy response.” Pharmacol Res.

Scherer, M., et al. (2020). "Quantitative Proteomics to Identify Nuclear RNA-Binding Proteins of Malat1." Int J Mol Sci 21(3).

Schlegelmilch, K., et al. (2011). "Yap1 acts downstream of alpha-catenin to control epidermal proliferation." Cell 144(5): 782-795.

Schmitt, A. M. and H. Y. Chang (2016). "Long Noncoding RNAs in Cancer Pathways." Cancer Cell 29(4): 452-463.

Schust, J., et al. (2006). "Stattic: a small-molecule inhibitor of STAT3 activation and dimerization." Chem Biol 13(11): 1235-1242.

Shao, D., et al. (2014). "A functional interaction between Hippo-YAP signalling and FoxO1 mediates the oxidative stress response." Nat Commun 5: 3315.

Shi, T., et al. (2016). "Long Noncoding RNAs as Novel Biomarkers Have a Promising Future in Cancer Diagnostics." Dis Markers 2016: 9085195.

Silvis, M. R., et al. (2011). "alpha-catenin is a tumor suppressor that controls cell accumulation by regulating the localization and activity of the transcriptional coactivator Yap1." Sci Signal 4(174): ra33.

Simoes, A. E., et al. (2015). "Aberrant MEK5/ERK5 signalling contributes to human colon cancer progression via NF-kappaB activation." Cell Death Dis 6(4): e1718.

Skibinski, A., et al. (2014). "The Hippo transducer TAZ interacts with the SWI/SNF complex to regulate breast epithelial lineage commitment." Cell Rep 6(6): 1059-1072.

Sohn, S. J., et al. (2008). "Non-redundant function of the MEK5-ERK5 pathway in thymocyte apoptosis." EMBO J 27(13): 1896-1906.

Sohn, S. J., et al. (2002). "ERK5 MAPK regulates embryonic angiogenesis and acts as a hypoxia-sensitive repressor of vascular endothelial growth factor expression." J Biol Chem 277(45): 43344-43351.

Spagnoli, F. M., et al. (1998). "Identification of a bipotential precursor cell in hepatic cell lines derived from transgenic mice expressing cyto-Met in the liver." J Cell Biol 143(4): 1101-1112.

Stecca, B. and E. Rovida (2019). "Impact of ERK5 on the Hallmarks of Cancer." Int J Mol Sci 20(6).

Sun, Q., et al. (2018). "Nuclear Long Noncoding RNAs: Key Regulators of Gene Expression." Trends Genet 34(2): 142-157.

Sun, R., et al. (2016). "Down-regulation of MALAT1 inhibits cervical cancer cell invasion and metastasis by inhibition of epithelial-mesenchymal transition." Mol Biosyst 12(3): 952-962.

Sun, Z., et al. (2019). "YAP1-induced MALAT1 promotes epithelial-mesenchymal transition and angiogenesis by sponging miR-126-5p in colorectal cancer." Oncogene 38(14): 2627-2644.

Tani, H., et al. (2010). "Stability of MALAT-1, a nuclear long non-coding RNA in mammalian cells, varies in various cancer cells." Drug Discov Ther 4(4): 235-239.

Tatake, R. J., et al. (2008). "Identification of pharmacological inhibitors of the MEK5/ERK5 pathway." Biochem Biophys Res Commun 377(1): 120-125.

Terasawa, K., et al. (2003). "Regulation of c-Fos and Fra-1 by the MEK5-ERK5 pathway." Genes Cells 8(3): 263-273.

Thum, T. and G. Condorelli (2015). "Long noncoding RNAs and microRNAs in cardiovascular pathophysiology." Circ Res 116(4): 751-762.

Tripathi, V., et al. (2010). "The nuclear-retained noncoding RNA MALAT1 regulates alternative splicing by modulating SR splicing factor phosphorylation." Mol Cell 39(6): 925-938.

Varelas, X. (2014). "The Hippo pathway effectors TAZ and YAP in development, homeostasis and disease." Development 141(8): 1614-1626.

Varelas, X., et al. (2010). "The Hippo pathway regulates Wnt/beta-catenin signaling." Dev Cell 18(4): 579-591.

Wang, K. C. and H. Y. Chang (2011). "Molecular mechanisms of long noncoding RNAs." Mol Cell 43(6): 904-914.

Wang, W., et al. (2015). "AMPK modulates Hippo pathway activity to regulate energy homeostasis." Nat Cell Biol 17(4): 490-499.

Wang, X., et al. (2005). "Targeted deletion of mek5 causes early embryonic death and defects in the extracellular signal-regulated kinase 5/myocyte enhancer factor 2 cell survival pathway." Mol Cell Biol 25(1): 336-345.

Wang, Y., et al. (2018). "TGF-beta-induced STAT3 overexpression promotes human head and neck squamous cell carcinoma invasion and metastasis through malat1/miR-30a interactions." Cancer Lett 436: 52-62.

Wang, Y., et al. (2016). "The Long Noncoding RNA MALAT-1 is A Novel Biomarker in Various Cancers: A Meta-analysis Based on the GEO Database and Literature." J Cancer 7(8): 991-1001.

Weldon, C. B., et al. (2002). "Identification of mitogen-activated protein kinase kinase as a chemoresistant pathway in MCF-7 cells by using gene expression microarray." Surgery 132(2): 293-301.

West, J. A., et al. (2014). "The long noncoding RNAs NEAT1 and MALAT1 bind active chromatin sites." Mol Cell 55(5): 791-802.

Wilson, K. E., et al. (2014). "PTPN14 forms a complex with Kibra and LATS1 proteins and negatively regulates the YAP oncogenic function." J Biol Chem 289(34): 23693-23700.

Wilusz, J. E., et al. (2008). "3' end processing of a long nuclear-retained noncoding RNA yields a tRNA-like cytoplasmic RNA." Cell 135(5): 919-932.

Woronicz, J. D., et al. (1995). "Regulation of the Nur77 orphan steroid receptor in activation-induced apoptosis." Mol Cell Biol 15(11): 6364-6376.

Xie, S. S., et al. (2016). "Emerging roles of non-coding RNAs in gastric cancer: Pathogenesis and clinical implications." World J Gastroenterol 22(3): 1213-1223.

Yan, C., et al. (1999). "Fluid shear stress stimulates big mitogen-activated protein kinase 1 (BMK1) activity in endothelial cells. Dependence on tyrosine kinases and intracellular calcium." J Biol Chem 274(1): 143-150.

Yang, Q., et al. (2010). "Pharmacological inhibition of BMK1 suppresses tumor growth through promyelocytic leukemia protein." Cancer Cell 18(3): 258-267.

Yang, Q. and J. D. Lee (2011). "Targeting the BMK1 MAP kinase pathway in cancer therapy." Clin Cancer Res 17(11): 3527-3532.

Yimlamai, D., et al. (2014). "Hippo pathway activity influences liver cell fate." Cell 157(6): 1324-1338.

Yin, F., et al. (2013). "Spatial organization of Hippo signaling at the plasma membrane mediated by the tumor suppressor Merlin/NF2." Cell 154(6): 1342-1355.

Shen Y, et al. (2021) “STAT3-YAP/TAZ signaling in endothelial cells promotes tumor angiogenesis. “Sci Signal. 14(712)

Yu, F. X., et al. (2012). "Regulation of the Hippo-YAP pathway by G-protein-coupled receptor signaling." Cell 150(4): 780-791.

Yu, W., et al. (2019). "Estrogen receptor beta promotes the vasculogenic mimicry (VM) and cell invasion via altering the

lncRNA-MALAT1/miR-145-5p/NEDD9 signals in lung cancer." Oncogene 38(8): 1225-1238.

Zanconato, F., et al. (2016). "YAP/TAZ as therapeutic targets in cancer." Curr Opin Pharmacol 29: 26-33.

Zanconato, F., et al. (2016). "YAP/TAZ at the Roots of Cancer." Cancer Cell 29(6): 783-803.

Zanconato, F., et al. (2015). "Genome-wide association between YAP/TAZ/TEAD and AP-1 at enhancers drives oncogenic growth." Nat Cell Biol 17(9): 1218-1227.

Zavadil, J. and E. P. Bottinger (2005). "TGF-beta and epithelial-to-mesenchymal transitions." Oncogene 24(37): 5764-5774.

Zen, K., et al. (2009). "ERK5 is a target for gene amplification at 17p11 and promotes cell growth in hepatocellular carcinoma by regulating mitotic entry." Genes Chromosomes Cancer 48(2): 109-120.

Zhang, N., et al. (2010). "The Merlin/NF2 tumor suppressor functions through the YAP oncoprotein to regulate tissue homeostasis in mammals." Dev Cell 19(1): 27-38.

Zhang, X., et al. (2017). "The long noncoding RNA Malat1: Its physiological and pathophysiological functions." RNA Biol 14(12): 1705-1714.

Zhang, X., et al. (2017). "MiR-101-3p inhibits the growth and metastasis of non-small cell lung cancer through blocking PI3K/AKT signal pathway by targeting MALAT-1." Biomed Pharmacother 93: 1065-1073.

Zhao, B., et al. (2008). "The Hippo-YAP pathway: new connections between regulation of organ size and cancer." Curr Opin Cell Biol 20(6): 638-646

Zhao, B., et al. (2007). "Inactivation of YAP oncoprotein by the Hippo pathway is involved in cell contact inhibition and tissue growth control." Genes Dev 21(21): 2747-2761.

Zheng, T., et al. (2018). "IL-8 Secreted from M2 Macrophages Promoted Prostate Tumorigenesis via STAT3" Int J Mol Sci. 2018 Dec 27;20(1):98.

Zhou, Y., et al. (2018). "Study on mechanism about long noncoding RNA MALAT1 affecting pancreatic cancer by regulating Hippo-YAP signaling." J Cell Physiol 233(8): 5805-5814.

Zong, X., et al. (2016). "Natural antisense RNA promotes 3' end processing and maturation of MALAT1 lncRNA." Nucleic Acids Res 44(6): 2898-2908.